JOURNAL OF THE MECHANICAL BEHAVIOR OF BIOMEDICAL MATERIALS 62 (2016) 139–157

Available online at www.sciencedirect.com

ScienceDirect

www.elsevier.com/locate/jmbbm

Review Article

An overview of multiphase cartilage mechanical modelling and its role in understanding function and pathology

Václav Klika[a,1,*], Eamonn A. Gaffney[b,1], Ying-Chun Chen[c], Cameron P. Brown[c]

[a]Department of Mathematics, FNSPE, Czech Technical University in Prague, Prague, Czech Republic
[b]Wolfson Centre for Mathematical Biology, Mathematical Institute, University of Oxford, Oxford, UK
[c]Nuffield Department of Orthopaedics, Rheumatology and Musculoskeletal Sciences, University of Oxford, Oxford, UK

ARTICLE INFO

Article history:
Received 22 December 2015
Received in revised form
15 April 2016
Accepted 25 April 2016
Available online 11 May 2016

Keywords:
Cartilage
Multiphase
Modelling
Structure
Function
Pathology

ABSTRACT

There is a long history of mathematical and computational modelling with the objective of understanding the mechanisms governing cartilage's remarkable mechanical performance. Nonetheless, despite sophisticated modelling development, simulations of cartilage have consistently lagged behind structural knowledge and thus the relationship between structure and function in cartilage is not fully understood. However, in the most recent generation of studies, there is an emerging confluence between our structural knowledge and the structure represented in cartilage modelling. This raises the prospect of further refinement in our understanding of cartilage function and also the initiation of an engineering-level understanding for how structural degradation and ageing relates to cartilage dysfunction and pathology, as well as informing the potential design of prospective interventions. Aimed at researchers entering the field of cartilage modelling, we thus review the basic principles of cartilage models, discussing the underlying physics and assumptions in relatively simple settings, whilst presenting the derivation of relatively parsimonious multiphase cartilage models consistent with our discussions. We proceed to consider modern developments that start aligning the structure captured in the models with observed complexities. This emphasises the challenges associated with constitutive relations, boundary conditions, parameter estimation and validation in cartilage modelling programmes. Consequently, we further detail how both experimental interrogations and modelling developments can be utilised to investigate and reduce such difficulties before summarising how cartilage modelling initiatives may improve our understanding of cartilage ageing, pathology and intervention.

*Corresponding author.
E-mail addresses: vaclav.klika@fjfi.cvut.cz (V. Klika), gaffney@maths.ox.ac.uk (E.A. Gaffney), cameron.brown@ndorms.ox.ac.uk (C.P. Brown).
[1]These authors contributed equally.

http://dx.doi.org/10.1016/j.jmbbm.2016.04.032

Contents

1. Introduction

Articular cartilage is found at opposing bone surfaces in joints and is a remarkable tissue, characterised by extremes of physiological structure and mechanical function: it lacks vasculature, lymphatics and nerves yet exhibits tribological properties that surpass engineering standards. With extremes of performance and loading over a whole lifetime, it is no surprise to find that articular cartilage function is both mechanically complex, and prone to degeneration and pathology.

The mechanical performance of cartilage is underpinned by its structure, as summarised in Fig. 1, which has been extensively documented (for instance by Athanasiou et al., 2013). The major constituents of cartilage include an anisotropic and heterogeneous matrix of predominantly type II collagen, intermeshed with high molecular weight proteoglycans, mainly aggrecans, immersed in an interstitial fluid containing numerous physiological electrolytes. Near the interface with bone, the collagen matrix is oriented predominantly perpendicular to the bone when averaged at the mesoscale, with average fibril orientation rotating on moving

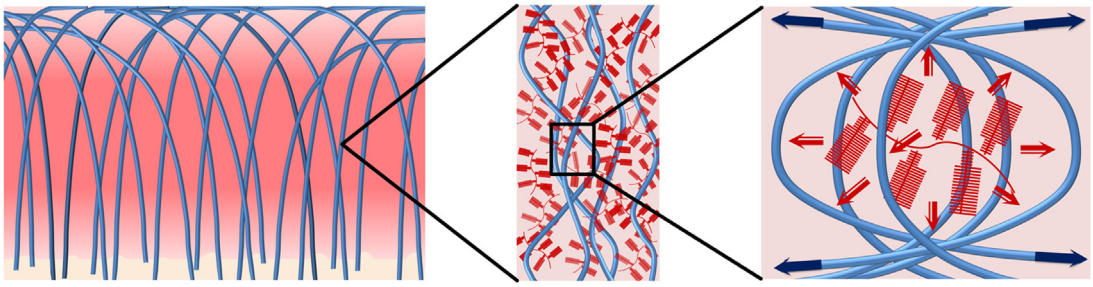

Fig. 1 – Hierarchical structure of articular cartilage, showing the organisation of collagen at different length scales from millimetre (left) to micrometre (right). On the left, the 'Benninghoff arcades' of collagen fibre orientation, which represents the predominant orientation of collagen fibrils on the mesoscale within a given region, is illustrated with bone at the bottom of the diagram. The typical distribution of aggrecan for the functional unit of load carriage is illustrated for healthy tissue in red (left), and its entanglement within the collagen meshwork, which is pseudo-random at lowers level of scale (centre and right). (For interpretation of the references to color in this figure caption, the reader is referred to the web version of thispaper.)

up through the cartilage until the fibrils are mainly parallel to the articulating surface, forming the classic 'Benninghoff arcades' (Benninghoff 1925). From theoretical studies, this mesoscale architecture is understood to ameliorate tissue stresses under load (Halonen et al., 2013), and enables a smooth transition of functionalities derived from microstructural effects.

At length scales of a few micrometres, the collagen orientation is pseudorandom, enabling the formation of an interconnected network that provides an effective entanglement of aggrecans (Maroudas, 1976; Broom and Oloyede, 1993; Brown et al., 2014). This interaction with aggrecans is of fundamental importance in the load bearing properties of joints. From a mechanical point of view, the large aggrecan macromolecules are deformed and compressed in the collagen network, forming a low-permeability composite structure that serves to retain fluid pressure, and provides compressive stiffness for cartilage. From an electrochemical point of view the aggrecans are relatively immobile, with a bottlebrush structure consisting of numerous glycoaminoglycan sidechains possessing electric charge, in turn inducing a shielding layer of electrophysiological ions, that is a Debye layer, and setting up ion concentration gradients and thus gradients of chemical potential. In turn, osmotic pressures act to reduce these ionic gradients, hydrating and thus swelling the solid cartilage constituent, placing the collagen under tensile stress (Maroudas, 1976; Ateshian, 2009). This overall tendency of the solid constituent to imbibe fluid is considered to have mechanical impact due to the induction of a pre-stress (Mow et al., 1999) and assisting in the prevention of cartilage being wrung out under load, especially in the context of recovery and repeated loading (Harrigan and Mann, 1987).

The detailed mechanisms of cartilage tribology during dynamic loading are similarly complex, as summarised in multiple reviews, which include Katta et al. (2008) and Ateshian (2009). Early advances in the understanding of cartilage lubrication were made by McCutchen (1959), who reported empirical evidence of weeping lubrication, drawing an analogy between cartilage and hydrated sponge, whereby loading induces solid constituent deformation together with fluid pressurisation and exudation, thus facilitating lubrication. An alternative hypothesis of boundary lubrication considered that load would compress the synovial fluid above the cartilage, ultra-filtering it, driving fluid into the cartilage and supporting lubrication via the remaining layer of lubricating synovial material, inducing boundary lubrication associated with closely opposing surfaces (Walker et al., 1968). The direction of flow under dynamic load appears to be difficult to empirically reconcile, whilst modelling frameworks can be found which support either concept (Hlavacek, 1993; Oloyede and Broom, 1996).

More recently, it has been emphasised that multiple lubrication modes can be exhibited by cartilage according to the detailed mechanical conditions (Gleghorn and Bonassar, 2008), with the primary mechanism for friction reduction due to fluid pressurisation, independent of flow direction (Katta et al., 2008). In this mechanism, elevated fluid pressure is primarily responsible for load bearing which in turn entails that fluid retains most of the load, so that the tribology of fluids, and thus low friction, dominates the interaction of opposing surfaces. However, with extended duration loads, the flow of fluid away from loaded regions inexorably decreases fluid pressurisation and thus increases load bearing by the solid matrix and consequently friction (Katta et al., 2008). This emphasises the need for combining proposed models at different scales via *multi-scale* modelling, in that larger spatial scales should be considered to have a theoretical representation of cartilage lubrication, whereby the far field conditions will be critical in fluid drainage routes and thus under what conditions and parameter regimes synovial fluid ultrafiltration may dominate interstitial fluid exudation and vice-versa.

The need to better understand joint pathology, and the role of mechanics in common and debilitating diseases such as osteoarthritis, bring further requirements. In particular, osteoarthritis initiation disrupts the complex balance between mechanics, structure and biology, and involves multiple tissues (Setton et al., 1999). Cartilage models must therefore look to higher levels of hierarchy to consider the wider mechanical environment of the joint and the influence from adjacent tissues such as bone and meniscus, and also look to lower levels to consider the scales at which damage and disease manifest. However, our understanding of the precise and complex mechanisms of cartilage structure–function relationships is incomplete. The knowledge that we do have is considered within the context of numerous, competing, computational modelling studies, in turn based on differing physical assumptions, making it difficult to translate model outputs to insight into disease and its treatment or prevention.

As cartilage modelling advances, there are increasing opportunities, and challenges, for its application in understanding the fundamental structure–function relationships in the tissue, and in particular their roles in disease and regeneration. Here, we aim to provide the modeller who is new to cartilage with an introduction to the field, its achievements, its uncertainties, and its main outstanding issues, including the scope for future opportunities in model validation and experimental comparison as part of using modelling and simulation as one of a complement of tools for improving our understanding of this complex tissue. Thus we first summarise the general concepts of these modelling frameworks together with their underlying assumptions, before focussing on how modelling has been evolving to improve our current and prospective future insights concerning cartilage. We continue by discussing open problems in boundary conditions for cartilage modelling that are inherited from multiphasic theories, as well as the need for modelling parametrisation and validation, whilst outlining how experimental interrogations of cartilage and modelling developments can support such a programme. Finally, we proceed to discuss how such developments in cartilage modelling can subsequently improve our understanding, especially in the context of pathology, ageing and intervention measures. However, the necessity of limiting scope entails there are many features of cartilage modelling that we do not consider in detail, particularly concerning the mechanical and hypoxic extremes of cartilage cells, chondrocytes, and their fundamental role in cartilage maintenance and remodelling.

Similarly, we do not discuss directly analogous multiphase models that are becoming popular in other areas of physiology, such as the mechanics of invertebrate discs and brain tissue (Karajan, 2012; Elkin et al., 2010).

2. A summary of general concepts within multiphase modelling frameworks for cartilage

Motivated by the fact simple media can be accurately described by the abstraction of a continuum at length scales significantly greater than the mean free path of the molecular constituents, there have been extensive investigations concerning whether and how the use of a continuum generalises for more complex media, such as mixtures of different fluids, solids with internal structure and of course biological tissue.

Within such models, constituents are defined to be the distinct species making up the media and among the simplest theories are the classical *mixture models* where the constituents are intermixed at molecular scales and equations are given in terms of balancing the mass fractions, momenta and energy of the constituents (e.g. Bowen and Eringen, 1976; Bowen, 1980; Bedford and Drumheller, 1983; Ateshian, 2007; Klika, 2014). Mixture theories can also be applied to media with immiscible constituents, which partition space into *phases* of distinct constituents even on lengthscales which are much greater than molecular (Bedford and Drumheller, 1983), generating *multi-phase* models. The properties of this phase-partition, typically expressed via the volume fractions for the phase of each constituent, enter the modelling framework which in general tracks both mass and volume fractions, requiring additional equations for the evolution of volume fractions. Fortunately interstitial fluid, like water, can be considered as incompressible under physiological conditions whilst the solid matrix of articular cartilage exhibits negligible volume changes with hydrostatic pressures up to 12 MPa (Bachrach et al., 1998). Hence the assumption of incompressible constituents is reasonable for cartilage, whereupon volume and mass fractions differ by only a constant and the miscible mixture theory framework has an equivalent mathematical structure to the multiphase framework. This entails that the crucial difference of how volume fractions are treated between many flavours of mixture and multiphase theories disappears, which encompasses diverse frameworks such as the microscale theories of miscible mixtures (Atkin and Craine, 1976; Bowen and Eringen, 1976; Truesdell, 1984; Lai et al., 1991; Müller and Ruggeri, 1998; Klika, 2014; Pavelka et al., 2014), the upscaled (averaged) theories of immiscible mixtures, the Theory of Porous Media (de Boer, 2005; Ehlers, 2002; Bercovici et al., 2001), the Hybrid Mixture Theory (Hassanizadeh and Gray, 1979; Bennethum and Cushman, 2002) or the Thermodynamically Constrained Averaging Theory (Gray and Miller, 2005).

However, a difference in the formulation of balance equations generally remains as these frameworks are considered on varying levels of description, with different or absent averaging procedures, and thus there is still a need to choose a modelling framework. Nonetheless, for cartilage tissue where constituents cannot be easily separated into phases at larger lengthscales even though the properties of each phase can be measured, such as interstitial fluid viscosity, mixture theory without averaging, which is equivalent to multiphase models given incompressible constituents, represents a self-consistent and appropriate modelling framework, in line with the works of Mow et al. or Ateshian et al.

In particular, since the general framework of all such mixture and multi-phase models consider constituents separately, the measurable properties of the phases can be defined and tracked so that their effect on bulk properties can be explored effectively. This link to physical properties, and the flexibility it allows, has considerable utility for understanding the complex mechanical consequences of known structural changes in a material such as cartilage. However, modelling uncertainties are likely to arise for the constitutive relations within such models, such as a specification of the stresses within the media in terms of deformation. Analogous remarks apply for the 'diffusive' drag forces between the different constituents (Bowen and Eringen, 1976; Bowen, 1980) and, in more complex media, relations such as how the osmotic stresses depend on ionic gradients in the presence of charged solutes.

Furthermore there are only weak guiding physical principles governing the a priori choice of these relations via the Second Law of Thermodynamics, that is no entropy destruction; this is often but not exclusively enforced using the classical Coleman-Noll procedure (Coleman and Noll, 1963) of Rational Thermodynamics (Truesdell, 1984), which ensures there is no pointwise entropy destruction at the microscale via the use of Lagrange multipliers. Nonetheless, other frameworks can be used, for example extended rational thermodynamics (Müller and Ruggeri, 1998; Wilmanski, 2008), which is based on rewriting the entropy inequality in a form that includes all field equations via Lagrange multipliers or, the approach used in hybrid mixture-theory, where the Second Law is enforced only for the macroscale-averaged version of the microscale equations. Thus there is considerable freedom, and difficulty, in this aspect of model building, though it is standard to use the most parsimonious constitutive relations consistent with the chosen enforcement of the Second Law.

Despite such difficulties, incompressible mixture models with the most parsimonious constitutive relations consistent with the Coleman–Noll procedure have generally enjoyed empirical success, especially in recent years with generalisations to include matrix heterogeneity, including depth-dependent material properties, and anisotropy, which are beginning to bring observed complex structure into cartilage models (e.g. Ateshian et al., 2009; Chen et al., 2006; Federico and Herzog, 2008; Guo et al., 2014; Moo et al., 2014; Pierce et al., 2013; Wilson et al., 2005a,b, 2006, 2007). All but a minority of these cartilage multiphase models are poroelastic, that is they represent a porous elastic network saturated with fluid, as initially developed by Biot in the context of pedology (Biot, 1941) and adapted for cartilage (Mow et al., 1980, 1989), with the later inclusion of the physicochemical properties of the aggrecans and electrolytes distinguishing cartilage models (e.g. Lai et al., 1991; Ateshian et al., 2009). Hence such models are our focus below, and we immediately note that they have been criticised under the assumption that the molecular level interweaving of solid matrix,

ions and interstitial fluid entails that multiple phases are inappropriate, and that instead a single cartilage phase should be used (Harrigan and Mann, 1987; Oloyede and Broom, 1996).

However, firstly note that the lengthscale of the cartilage matrix void, at its smallest is the separation between glycoaminoglycan chains on aggrecans which, for mature cartilage, is 4.4($\pm$1.2) nm (Ng et al., 2003) and secondly note that the hydrodynamics of water appears to be a reasonable approximation down to scales of 10 molecular diameters (Travis et al., 1997), or about three nanometres (Soper and Benmore, 2008), though discrepancies occur at one molecular diameter from a boundary, consistent with a breakdown of the no-slip boundary condition. Thus, neglecting this region of the domain, one may conclude that treating fluid as a separate phase in cartilage is (tolerably) consistent with continuum fluid dynamics. In addition, the mechanics of single constituents of the solid matrix at the lowest structural level that need be considered, such as that of a collagen fibril, can be described in terms of continuum principles such as stiffness so that the solid matrix can be described as a continuum phase[2]. Thus, there appears to be no physical principle on which to a-priori distinguish a single phase model over a multi-phase model. Furthermore, whilst the use of a single phase model is attractive in terms of tractability and the prospect of the improved insight this may bring, assuming modelling accuracy can be maintained, the scope of such models in parameter space is severely limited by the extent to which the hard-wired single phase constitutive relations retain validity as the ratios of the constituents change. In particular, single-phase frameworks do not track the fundamental constituents and thus do not automatically allow for how a change in constituents would impact the constitutive relations.

In contrast, the multiphase/mixture framework offers the prospect of a theory that is more adaptive, with the potential to maintain predictive power in larger regions of parameter space, for example, with changes in proteoglycan densities, subject to the final arbiter of experiment. Given the existing validation of the poroelastic models (e.g. Mow et al., 1980, 1989; Ateshian et al., 1997; Wilson et al., 2005a,b; Ateshian et al., 2009), increased versatility is suggested as an overriding requirement in using models to improve our understanding of cartilage, especially in the parameter extremes of pathology. Thus in the following section we provide a detailed summary of multiphase poroelastic models of cartilage and the extent to which these models can be simplified, as well as briefly considering recent developments in multiphase and mixture theory frameworks, before exploring the prospects of relating cartilage modelling to observations and for understanding pathology.

[2]At least given the matrix network allows an averaging of its structure so that this structure can be described in terms of macroscopic variables, as implicitly assumed throughout both single phase and multi-phase cartilage modelling

3. Multiphase models

We begin by detailing and deriving the formulation of a core biphasic model, representing the solid and fluid phases of cartilage, before introducing the effect of osmotic pressures and examining boundary conditions. We then survey possible extensions to represent cartilage structure in more extensive detail, such as the inclusion of collagen fibre anisotropies.

3.1. *Biphasic poroelastic models*

The simplest poroelastic cartilage framework is the *biphasic model* (Mow et al., 1980, 1986), with two constituents, the solid matrix and interstitial fluid, which in combination fill space, and this framework reduces to the classical Biot model (Biot, 1941) for infinitesimal strain (Bowen, 1980). We will briefly summarise a formulation of a biphasic model: as already discussed above, continuum fluid dynamics is legitimate for the interstitial phase fluid dynamics, and thus we use continuum fluid dynamics, deviating from the traditional frameworks (Mow et al., 1980, 1986; Lai et al., 1991; Huyghe and Janssen, 1997) though the resulting framework is, at most, a simple variant of the standard biphasic model and any differences are in principle testable.

3.1.1. *Mass and momentum balance*

By microscale incompressibility, we have that the mass densities ρ^{f} and ρ^{s} for the fluid and solid phases, are related to their volume fractions $\phi^{\mathrm{f}}, \phi^{\mathrm{s}}$ by the constant, true, density of the phases, via $\rho_{\mathrm{T}}^{\beta}\phi^{\beta}=\rho^{\beta}$, with $\beta\in\{f,s\}$ and where the T subscript denotes true density. In addition, demanding the material fills all space yields

$$1=\phi^{\mathrm{f}}+\phi^{\mathrm{s}}. \tag{1}$$

furthermore, we have velocity fields of the fluid phase, denoted by $\boldsymbol{v}^{\mathrm{f}}$, and the displacement of solid phase material points $\boldsymbol{u}^{\mathrm{s}}(\boldsymbol{X},t)=\boldsymbol{x}(\boldsymbol{X},t)-\boldsymbol{X}$, where $\boldsymbol{x}(\boldsymbol{X},t)$ maps material points, $\boldsymbol{X}$ in the reference configuration to points $\boldsymbol{x}$ in the inertial frame at a given time, t; these represent 6 unknown scalar fields. We enforce constraint (1) using a Lagrange multiplier, denoted p, via the Coleman–Noll procedure (Coleman and Noll, 1963), as detailed in Section 1 of the Electronic Supplementary Material (ESM). We thus have 9 macroscale scalar unknowns, $\{\boldsymbol{u}^{\mathrm{s}},\boldsymbol{v}^{\mathrm{f}},p,\phi^{\mathrm{f}},\phi^{\mathrm{s}}\}$, and hence 9 scalar equations are required, of which constraint (1) is one. Two more scalar equations arise from mass balances, with a further six from the balance of momentum.

With the assumptions of mixture theory for porous media (Bowen, 1980), equivalent to a multiphase model given constituent incompressibility, we have the *macroscale* mass balances

$$\frac{\partial\rho^{\beta}}{\partial t}+\frac{\partial}{\partial x_{\mathrm{i}}}\left(\rho^{\beta}v_{\mathrm{i}}^{\beta}\right)=0,\quad \beta\in\{\{f,s\}\}, \tag{2}$$

where $\boldsymbol{v}^{\mathrm{s}}:=D\boldsymbol{u}^{\mathrm{s}}/Dt$, $\rho_{\mathrm{T}}^{\beta}\phi^{\beta}=\rho^{\beta}$ and where $\partial/\partial t$ holds $\boldsymbol{x}$, a point in the inertial reference frame, fixed in contrast to the derivative D/Dt, which is relative to a material point, denoted $\boldsymbol{X}$, fixed in the reference configuration of the solid phase.

In formulating the momentum balance equations, we assume the system is isothermal and with negligible inertia, as motivated in the ESM, Section 2. Further noting, as implicit in the mixture theory framework, that all stress gradients and drag forces are defined *per unit volume of tissue*, mixture theory postulates the following form of the *macroscale* equations

$$\frac{\partial \sigma^{\mathrm{f}}_{ij}}{\partial x_j} + q^{\mathrm{f}}_i = 0, \quad \frac{\partial \sigma^{\mathrm{s}}_{ij}}{\partial x_j} + q^{\mathrm{s}}_i = 0,$$
$$\boldsymbol{q}^{\mathrm{f}} = -\boldsymbol{q}^{\mathrm{s}} = \gamma(\boldsymbol{v}^{\mathrm{s}} - \boldsymbol{v}^{\mathrm{f}}) + \Delta \boldsymbol{q}. \tag{3}$$

Here $\boldsymbol{\sigma}^f, \boldsymbol{\sigma}^{\mathrm{s}}$ are the Cauchy stress tensors for the elastic and solid phases and $\boldsymbol{q}^{\mathrm{f}}$ is the stress exerted on the fluid phase by the solid phase, with $\boldsymbol{q}^{\mathrm{f}} = -\boldsymbol{q}^{\mathrm{s}}$ by Newton's Third Law. A standard choice for this term is $\gamma(\boldsymbol{v}^{\mathrm{s}} - \boldsymbol{v}^{\mathrm{f}})$, with $\gamma > 0$ constant (Mow et al., 1980, 1986; Huyghe and Janssen, 1997; Wilson et al., 2005a,b; Julkunen et al., 2013). However, this immediately discounts how the detailed structure impacts the relative forces between the two phases and, once more, information about cartilage structure is lost. Finally, we additionally require an additional drag term, $\Delta \boldsymbol{q}$ to enforce thermodynamic consistency, as detailed in the ESM, Section 1.

3.1.2. *Constitutive relations*

To close the above equations, we firstly require a specification of the fluid stress in terms of the rate of fluid strain and the solid stress in terms of deformation, assuming each phase is respectively an incompressible viscous fluid and an incompressible hyperelastic solid. We additionally require a specification of $\Delta \boldsymbol{q}$ to define the inter-phase drag. A common assumption more generally is that the constitutive relation of the pure material is inherited by each constituent in proportion to its volume fraction (Bedford and Drumheller, 1983), though a priori there is no guarantee that this is consistent with thermodynamics and requires careful consideration (see e.g. Huyghe et al., 2009). Here, our choices are the most parsimonious that are consistent with the constraint $\phi^{\mathrm{s}} + \phi^{\mathrm{f}} = 1$ and the Second Law of Thermodynamics.

As derived in detail in the ESM, Section 1, via the Coleman–Noll procedure (Coleman and Noll, 1963) we have that the fluid phase constitutive relation depends on ϕ^f, the rate of strain tensor

$$D_{ij} = \frac{1}{2}\left(\frac{\partial v^f_i}{\partial x_j} + \frac{\partial v^f_j}{\partial x_i}\right) \tag{4}$$

and the Lagrange multiplier for the constraint $\phi^{\mathrm{s}} + \phi^{\mathrm{f}} = 1$, denoted $p(\mathbf{x}, t)$, via

$$\boldsymbol{\sigma}^f = -\phi^{\mathrm{f}} p \boldsymbol{I} + 2\mu\left(\boldsymbol{D} - \frac{1}{3}[\mathrm{tr}\boldsymbol{D}]\boldsymbol{I}\right), \tag{5}$$

where $\boldsymbol{I}$ is the identity and with $\mu > 0$ physically interpreted as viscosity. Note that this constitutive relation does not prevent $\nabla \cdot \boldsymbol{v}^{\mathrm{f}} \neq 0$, for example as fluid is exuded from a region. Thus, the fluid flow is not that of a single phase incompressible fluid, even though on the microscale the fluid is assumed to be incompressible. There is no inconsistency, as discussed in detail in the ESM, Section 3, and these remarks also apply to the solid phase constitutive relation.

To consider the solid phase constitutive relation in detail, let ψ be the solid phase free energy per unit volume of the reference configuration; the ability to associate a free energy in this manner is an implicit assumption, of *hyperelasticity*, on the solid phase, which in itself should be subjected to empirical testing. With this assumption then, akin to the energy of a Hookean spring, the solid phase free energy is written in terms of deformation. Given material isotropy and the requirement that the material properties be independent of the reference frame, this can be considered, without loss of generality (Gurtin et al., 2010), in terms of the right Cauchy–Green deformation tensor $\mathbf{C} = \boldsymbol{F}^T\boldsymbol{F}$ where $\boldsymbol{F}$ is the deformation tensor, given by

$$F_{ij} = I_{ij} + \frac{\partial u^{\mathrm{s}}_i}{\partial X_j} = \frac{\partial x_i}{\partial X_j}. \tag{6}$$

Then the Coleman–Noll procedure, as detailed in the ESM, Section 1, entails that

$$\boldsymbol{\sigma}^{\mathrm{s}} = -\phi^{\mathrm{s}} p \boldsymbol{I} + \frac{2}{\det \boldsymbol{F}} \boldsymbol{F} \frac{\partial \psi(\mathbf{C})}{\partial \mathbf{C}} \boldsymbol{F}^T. \tag{7}$$

Note that there are numerous possible explicit such forms for ψ, for instance neo-Hookean or Mooney–Rivlin free energies (Gurtin et al., 2010) but the distinction between these choices forms part of the difficult aspect of parametrising the constitutive relation for cartilage, which we discuss further below.

Finally we have from the Coleman–Noll procedure that the simplest thermodynamically consistent form of $\Delta \boldsymbol{q}$ within the above modelling formulation is given by $\Delta \boldsymbol{q} = p\nabla\phi^{\mathrm{f}} = -p\nabla\phi^{\mathrm{s}}$. Thus in summary we have the full set of nine equations that are given by $\phi^{\mathrm{s}} + \phi^{\mathrm{f}} = 1$, the two mass balances of Eq. (2) and the six scalar momentum balances

$$-\phi^{\mathrm{f}}\nabla p + \gamma\left(\boldsymbol{v}^{\mathrm{s}} - \boldsymbol{v}^{\mathrm{f}}\right) + \mu\left[\nabla^2_{\mathbf{x}}\boldsymbol{v}^{\mathrm{f}} + \frac{1}{3}\nabla_{\mathbf{x}}\left(\nabla_{\mathbf{x}} \cdot \boldsymbol{v}^{\mathrm{f}}\right)\right] = \boldsymbol{0}, \tag{8}$$

$$-\phi^{\mathrm{s}}\nabla p + \nabla_{\mathbf{x}} \cdot \left\{\frac{2}{\det \boldsymbol{F}} \boldsymbol{F} \frac{\partial \psi(\mathbf{C})}{\partial \mathbf{C}} \boldsymbol{F}^T\right\} + \gamma\left(\boldsymbol{v}^{\mathrm{f}} - \boldsymbol{v}^{\mathrm{s}}\right) = \boldsymbol{0}. \tag{9}$$

In the above, note that the pressure is the isotropic stress and respectively given for the fluid and solid phases via

$$-\frac{1}{3}\mathrm{tr}\boldsymbol{\sigma}^f, \quad -\frac{1}{3}\mathrm{tr}\boldsymbol{\sigma}^{\mathrm{s}};$$

in particular, and in contrast to a single-phase Newtonian fluid, the pressure is not equivalent to a constraint Lagrange multiplier. Noting that the phase densities and volume fractions are constant multiples of each other, the nine scalar bulk biphasic Eqs. (1), (3), (8), (9) constitute a closed model where the boxed viscosity terms have the prospect of being subordinate since the viscous scales are often small, as discussed in the ESM, Section 2. However, the neglect of such viscous terms constitutes a singular perturbation and thus, in generality, these terms may need to be retained, in which case they induce boundary layer effects; otherwise Eq. (8) reduces to simply a D'Arcy law for the flow of the fluid relative to the solid phase.

We remark that while this framework is commonplace it does not retain physical consistency should either of the volume fractions approach zero. Then the stresses and inter-phase stresses per unit volume of tissue do not tend to zero, implying a finite force on an infinitesimal amount of medium and hence theory breakdown. Strictly, one should implement the replacement $\boldsymbol{q}^j \to \phi^{\mathrm{s}}\phi^{\mathrm{f}}\boldsymbol{q}^j, j \in \{f, \mathrm{s}\}$ so that momentum

exchange tends to zero if either volume fraction tends to zero. In addition the stresses should be weighted by ϕ^f for the fluid and ϕ^s for the solid so that neither phase contributes a stress in the limit that it is exuded, i.e. the choice of the anisotropic stresses chosen via the Collman–Noll procedure become

$$\left(\boldsymbol{\sigma}^j - \frac{1}{3}\mathrm{tr}\boldsymbol{\sigma}^j\mathbf{I}\right) \to \phi^j\left(\boldsymbol{\sigma}^j - \frac{1}{3}\mathrm{tr}\boldsymbol{\sigma}^j\mathbf{I}\right), \quad j \in \{\{f, s\}\}.$$

The consequences of this constitute a straightforward exercise to derive by generalising the calculations of the ESM, Section 1, though we only have derived the classical models for reasons of brevity. This more generally emphasises the importance of model testing to distinguish whether such model variations are important in the physiological or pathological regime.

Finally, one should note that any biphasic model fails to capture various aspects of cartilage behaviour, for example cartilage microstructure and the influence of changes in osmotic pressure, limiting utility for disease-related modelling, due to the importance of physicochemical and structural effects. Thus we proceed to describe modelling generalisations below.

3.2. *Triphasic and quadphasic poroelastic models*

The classical work of Lai et al. (1991) could be considered as founding the *triphasic* modelling framework for cartilage, generalising biphasic models by incorporating an ionic phase. This yields complex models that allow for a tighter link between the actual observed processes and the modelling representation, which can be reflected in simpler constitutive relations as contributions to overall behaviour are linked to individual constituents. Nonetheless triphasic treatments, with the solid phase of tissue simplified to a homogeneous, isotropic, linearly elastic material undergoing infinitesimal strain, can often be related to biphasic models a posteriori in contexts where the properties of the aggrecans do not change extensively (Ateshian et al., 2004).

Further generalisations appear with the *quadphasic* description of cartilage tissue, as proposed by Huyghe and Janssen (1997), with cations and anions treated separately in order to capture swelling more accurately. General treatments for an arbitrary number of ion species can be found in Gu et al. (1998) and in Ateshian's analysis (Ateshian, 2007). The latter work can be considered as the most comprehensive and general treatment of soft tissue modelling based on mixture theory and rational thermodynamics; it also includes a modelling description of phenomena such as growth or reactions among constituents and simplifying assumptions for cartilage and soft tissue modelling are discussed and implemented.

3.2.1. *On the triphasic model*

We proceed to consider the biophysics of physiological ion dynamics, though with some deviations from traditional triphasic frameworks (Mow et al., 1980, 1986; Lai et al., 1991; Huyghe and Janssen, 1997). In particular, we build upon the biphasic model of the previous section and thus inherit its differences. In addition we briefly consider ion transport via the *generalised* Stefan-Maxwell equations (Quintard et al., 2006), which extend the kinetic theory momentum balances of perfect gas mixtures to fluids (Lightfoot et al., 1962) and reduce to the standard, Fickian, diffusion equation for a single solute (Quintard et al., 2006). Within approximately two Debye lengths (Moy et al., 2000; Corry et al., 2000) from charges fixed on the aggrecans of the solid phase, the violation of electroneutrality also needs to be considered as it induces an osmotic swelling pressure, which can have very important mechanical effects in cartilage. We also note that effects such as entropic and excluded volume contributions to the ion-induced pressures are not considered here to maintain model simplicity. In particular, a number of modelling studies have incorporated these influences, such as Lai et al. (1991) and this is likely to be important at relatively low fixed charge densities, especially in the pathological regime.

Ion transport: As with most other modelling frameworks we only consider sodium and chloride ions with c^+ the sodium ion concentration, *defined per unit volume of fluid (rather than per unit volume of tissue)* and c^- the chloride ion concentration. In the bulk we have $c^+ = c^- := c$ by electroneutrality. Thus the above biphasic formulation is still valid and we simply require a coupling between the forces associated with the Debye layers and the biphasic model, and Donnan theory is typically used (Mow et al., 1986; Lai et al., 1991; Huyghe and Janssen, 1997).

However, under physiological conditions a Debye length is about one 0.5–1 nm (Moy et al., 2000; Weiss, 1996), which entails Debye layers from adjacent glycoaminoglycans on the brush-structure of aggrecan can potentially interact; such interactions are not captured in Donnan theory, which is also unreliable at physiological isotonicity (Basser and Grodzinsky, 1993). The Poisson–Boltzmann equation framework, or the equivalent results of the Poisson–Nernst–Planck equation framework (Weiss, 1996), are more fundamental and can capture the impact of overlapping Debye layers, as explored by Buschmann et al. (1995), who also present an empirical study favouring this more general theory. Nonetheless, below we restrict ourselves to Donnan theory to determine the osmotic swelling pressure, p^{Swell}, in terms of the bulk, electroneutral concentration, c, and the fixed charge density, with latter given in terms of the initial distribution of fixed charge density, assumed to be known.

Hence, to proceed we consider the ion transport equation at the *microscale* level

$$\frac{\partial c}{\partial t} = \nabla(D \cdot \nabla c) - \nabla \cdot \left(c\boldsymbol{v}^f_{micro}\right), \tag{10}$$

where D is the diffusion coefficient of NaCl and $\boldsymbol{v}^f_{micro}$ is the flow field at the microscale. Thus $\nabla \cdot \boldsymbol{v}^f_{micro} = 0$ by incompressibility; physiologically at least typical boundary conditions will simply be zero ionic flux at domain boundaries and the initial condition would be isotonicity. Under these conditions, constant, isotonic, c is *the solution in the bulk*. This can be understood intuitively: at very small scales within cartilage pores diffusion is very effective and dominates transport and acts to drive the solute to its mean concentration, and thus c is approximately constant (at least once transients have decayed which happens on short timescales within a cartilage pore). Of course in experimental investigations, for

instance placing excised cartilage in a salt bath to assess swelling, one can readily find conditions when solute transport is non-trivial. However, this requires boundary conditions that strongly force the solution and we do not address these extremes and this assumption of ionic equilibrium also features in the literature for example, in the framework introduced by Wilson and co-workers (Wilson et al., 2005a, b, 2006, 2007); it also entails the model presented below is often referred to as *the biphasic swelling model* rather than a full triphasic model (Wilson et al., 2005a,b).

The mechanical impact of ions: Via the Donnan theory for a binary solution of monovalent electrolytes, the osmotic swelling pressure is predicted to be

$$p^{Swell} = RT\left(\sqrt{c_f^2 + c_b^2} - c_b\right), \tag{11}$$

where R is the gas constant, T is temperature and $c_b = 2c$ is the osmolarity of the bulk interstitial fluid away from Debye layers and c_f is the fixed charge density, noting that some authors additionally consider further corrections in terms of a polynomial expansion obtained from experimental measurements, see Ateshian et al. (2009). Thus the ion concentration, c, in the bulk, as can be determined from the above allows the ready determination of the Donnan osmotic, or swelling, pressure thus providing an expression for the macroscopic pressure gradient due to physiological ions and fixed charges, denoted $\nabla_{\mathbf{x}}(p^{Swell})$ below (Lai et al., 1991; Huyghe and Janssen, 1997; Ateshian, 2007).

We inherit the constitutive laws of the biphasic model and assume linear constitutive laws without cross terms for ion transport, as is typically observed for ion transport (e.g. Chapter 1, Bachelor 2000), and exemplified by the above assumption of Fickian diffusion in the bulk within Eq. (10). Thus for instance we do not consider the possibility of a chemical expansion stress (Huyghe et al., 2009), though this would be an interesting generalisation. With these assumptions the derivation of the bulk equations, including the Coleman–Noll procedure, proceeds as previously, as detailed in the ESM, Section 1, and we have

$$1 = \phi^f + \phi^s \tag{12}$$

$$0 = \frac{\partial \phi^{\mathrm{f}}}{\partial t} + \mathrm{div}\left(\phi^{\mathrm{f}}\mathbf{v}^{\mathrm{f}}\right) = \frac{\partial \phi^{\mathrm{s}}}{\partial t} + \mathrm{div}(\phi^{\mathrm{s}}\mathbf{v}^{\mathrm{s}}), \tag{13}$$

$$\begin{aligned} \mathbf{0} = &-\phi^{\mathrm{f}}\nabla_{\mathbf{x}}p + \gamma\left(\mathbf{v}^{\mathrm{s}} - \mathbf{v}^{\mathrm{f}}\right) - \phi^{\mathrm{f}}\nabla_{\mathbf{x}}p^{Swell} \\ &+ \mu\left[\nabla_{\mathbf{x}}^2\mathbf{v}^{\mathrm{f}} + \frac{1}{3}\nabla_{\mathbf{x}}\left(\nabla_{\mathbf{x}}\cdot\mathbf{v}^{\mathrm{f}}\right)\right], \end{aligned} \tag{14}$$

$$\mathbf{0} = -\phi^{\mathrm{s}}\nabla_{\mathbf{x}}p + \nabla_{\mathbf{x}}\cdot\left\{\frac{2}{\det \mathbf{F}}\mathbf{F}\frac{\partial \psi(\mathbf{C})}{\partial \mathbf{C}}\mathbf{F}^T\right\} + \gamma\left(\mathbf{v}^{\mathrm{f}} - \mathbf{v}^{\mathrm{s}}\right), \tag{15}$$

where the Donnan swelling pressure is given by

$$p^{Swell} = RT\left(\sqrt{c^2 + c_b^2} - c_b\right). \tag{16}$$

Once more, the fluid viscosity terms are boxed as they have the potential to be neglected apart from the possibility of boundary layers.

For either the biphasic or the biphasic swelling/triphasic models one also needs to consider initial conditions, which are generally straightforward, and boundary conditions, which can be complex and hence we proceed to discuss these conditions in detail.

3.3. *Boundary and initial conditions*

Boundary conditions are equally important in any mathematical formulation of a given problem and corresponding attention is required. Yet, despite all the development in the field of mixture theories, and even more so for averaging theories, the problem of plausible boundary conditions for constituent variables remains an open question.

In particular, difficulties generally arise because physical principles require total balances at interfaces, for example the balance of mass and momentum, but the partition of mass and momentum among the various phases at a boundary for mixture and multiphase media that is required for system closure is not subject to the same physical requirements, and thus can require additional justification or assumption. Tangential stress conditions are particularly problematic and have been considered in pioneering experimental and modelling work by Beavers and Joseph, exploring the boundary conditions between fluid and porous media (Beavers and Joseph, 1967). This study illustrated that a boundary layer formed at the interface of a viscous fluid and a porous medium, a special case of a multiphase model, and hence one cannot simply neglect viscosity in general for multiphase and mixture models, including those used to represent cartilage. In additional, detailed theoretical justifications of the Beavers and Joseph condition (Beavers and Joseph, 1967) have been presented by Saffman (1971) and more recently by Chandesris and Jamet (2006), though deformation of the solid phase is not considered.

In the context of cartilage, Hou et al. (1989) proposed a hypothesised kinematic condition, which gave a tangential stress boundary condition and studied its implications for solutions of biphasic cartilage model. Although their results are promising, the problem of boundary conditions for bi- and tri-phasic models is not solved here in that one still has only a hypothesised boundary condition. Lai et al. (1991) further highlight that the continuity of chemical potentials is required, whilst Ateshian et al. (1994) uses the results of Hou et al. (1989) and modifies them for frictionless contact between two biphasic layers whose fluid phase is inviscid with zero tangential surface stress $\mathbf{t}.eag\sigma.\mathbf{n} = 0$, where $\boldsymbol{\sigma}$ stands for total stress defined in the ESM, Section 1.

More generally, Rajagopal (2007) noted that the decomposition of boundary conditions of a mixture into boundary conditions of constituents is likely dependent on the particular problem at hand and calls for developing a constitutive theory. Surprisingly, this study also reports that there is an insensitivity to the detailed decomposition of boundary conditions among the different phases. In particular (i) saturated boundary conditions, (ii) a decomposition of traction among constituents based on volume fractions and (iii) a decomposition based on the requirement for constant chemical potential across boundary all yielded similar, plausible, results in the context of fluid flow past a slab. Nonetheless, the appropriate choice of boundary condition is far from settled. Finally, the recent work by Dell'Isola et al. (2009) approaches the issue of biphasic model boundary conditions

via a variational approach and seems to be a promising treatment of this issue, even allowing the incorporation of friction or dissipation.

In light of such uncertainties, we conclude this section by discussing the unambiguous boundaries conditions of a simple 1d problem for cartilage and also the higher dimensional case of a joint, where we explicitly use the Beavers–Joseph framework to hypothesise relevant BCs for cartilage models, whilst calling for experimental guidance concerning tangential components of velocities.

3.3.1. *One dimensional experiments*

Before proceeding note that the above triphasic model has an isotonic ion concentration in the bulk, given the assumption this is consistent with the boundary conditions. In practice this means the cartilage is not subject to large ionic concentration gradients, which occur only in experimental settings, such as an immersion in a salt bath. Hence the initial and boundary conditions below are sufficient for both the biphasic and triphasic models discussed above.

The simplest scenario to consider is a one-dimensional compression of cartilage with a porous filter plunger, at $z = z_*(t) > 0$, and a rigid impermeable base at $z = 0$ (Mow et al., 1986), as depicted in Fig. 2. Reducing fields to one spatial dimension, for instance,

$$\boldsymbol{v}^f(\boldsymbol{x}, t) \to \boldsymbol{e}_z v^f(z, t),$$

where $\boldsymbol{e}_z$ is the z-direction unit vector, typical boundary conditions would be

$$\boldsymbol{v}^f(0, t) = \boldsymbol{v}^s(0, t) = \boldsymbol{0}, \quad \boldsymbol{v}^s(z_*(t), t) = \dot{z}_*(t)\boldsymbol{e}_z,$$
$$\boldsymbol{\sigma}^f(z_*(t), t)\boldsymbol{e}_z = -\left[P_{atm} - \frac{8\mu l \dot{z}_*(t)}{a^2} + \rho g l\right]\boldsymbol{e}_z,$$

where the fluid has density ρ, viscosity μ and the plunger has identical cylindrical pores of height l and radius a. In particular, in addition to atmospheric pressure, there are contributions due to hydrostatic pressure ($\rho g l$) and a Poiseuille flow pressure drop, neglecting any entry flows complications in the pores, which is reasonable at low Reynolds number providing the pore radius is much less than its length (Goldberg and Folk, 1988). More generally for sufficiently slow flow and shallow pores, such terms are negligible. Hence, in this model the solid phase is advected with the porous plunger but the fluid phase satisfies a stress balance. Initial conditions would typically be

$$\boldsymbol{v}^f(z, 0) = \boldsymbol{v}^s(z, 0) = 0,$$

provided $\dot{z}_*(0) = 0$ to ensure consistency between the boundary and initial conditions. In particular this model has been investigated in detail, where atmospheric pressure dominates other pressure terms, by Mow et al. (1986).

3.3.2. *Multiple spatial dimensions*

In multiple dimensions, and/or in the context of joints, boundary conditions have been stipulated and hypothesised by Hou et al. (1989), and are fundamentally important in understanding cartilage behaviour. In particular for physiological, in vivo modelling the histological scale necessarily couples with the anatomical scale, as required to ascertain overall fluid motion and thus the details of cartilage tribology.

As an exemplar, we consider the joint of a finger pressed against a hard surface, as illustrated in Fig. 3, thus imposing a pressure, $p^*(t)$, at the upper bone-cartilage interface. The synovial fluid is represented via a stress tensor $\boldsymbol{\sigma}^{Synovial}$ and a velocity field, $\boldsymbol{v}^{Synovial}$, which here is simplified to that of a Newtonian fluid, though in practice synovial fluid is viscoelastic (Thurston and Greilin, 1978). Whilst an anatomically accurate model would not possess symmetry, axisymmetry presents an opportunity for moderate simplification, as illustrated in Fig. 3. Even this simple case of a finger knuckle is geometrically complex, requiring closure from the deformation of the fibrous capsule. This could, for instance, be modelled as a stiff shell, with velocity and stress continuity boundary conditions for the free boundary, i.e.

$$\boldsymbol{\sigma}^{Synovial} \cdot \boldsymbol{n} = \boldsymbol{\sigma}^{shell} \cdot \boldsymbol{n}, \quad \boldsymbol{v}^{Synovial} = \boldsymbol{v}^{shell},$$

where $\boldsymbol{\sigma}^{shell}$, $\boldsymbol{v}^{shell}$ are the stress and velocity fields of the shell and $\boldsymbol{n}$ generically in this section is a unit normal to the interface where the boundary condition is imposed. Suitable initial conditions for the finger joint model are straightforward; for instance the initial state of the system could be unloaded, whereafter $p^*(t)$ is increased to represent loading of the finger.

Cartilage Boundary conditions: The boundary conditions for the cartilage, modelled as a bi- or tri- phasic material, are more vexatious to specify. Firstly, note that the solid phase moves with the cartilage boundary so characteristics of the solid phase velocity do not enter the cartilage domain and hence no boundary conditions are required for the equation governing the solid phase mass balance. However, if there is a flux of fluid into the cartilage, then a flux boundary

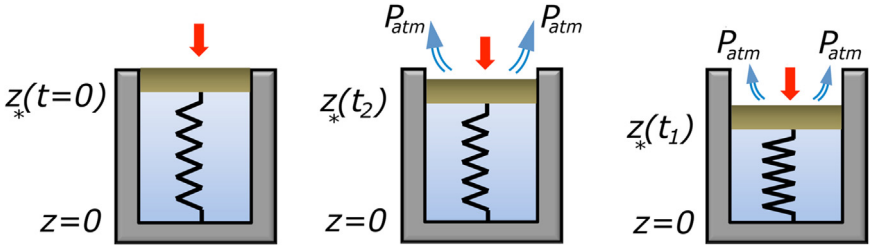

Fig. 2 – A schematic of the plunger experiment and its boundary conditions. Cartilage (blue) is compressed from time $t = 0$ in the z-direction with a porous plunger (brown). The fluid phase is exuded (blue arrows) at equilibrium with atmospheric pressure, P_{atm} while the solid phase is condensed between impermeable walls (grey) and the plunger, whose position $z_*(t)$, at times $t_2 > t_1 > 0$ is depicted. (For interpretation of the references to color in this figure caption, the reader is referred to the web version of this paper.)

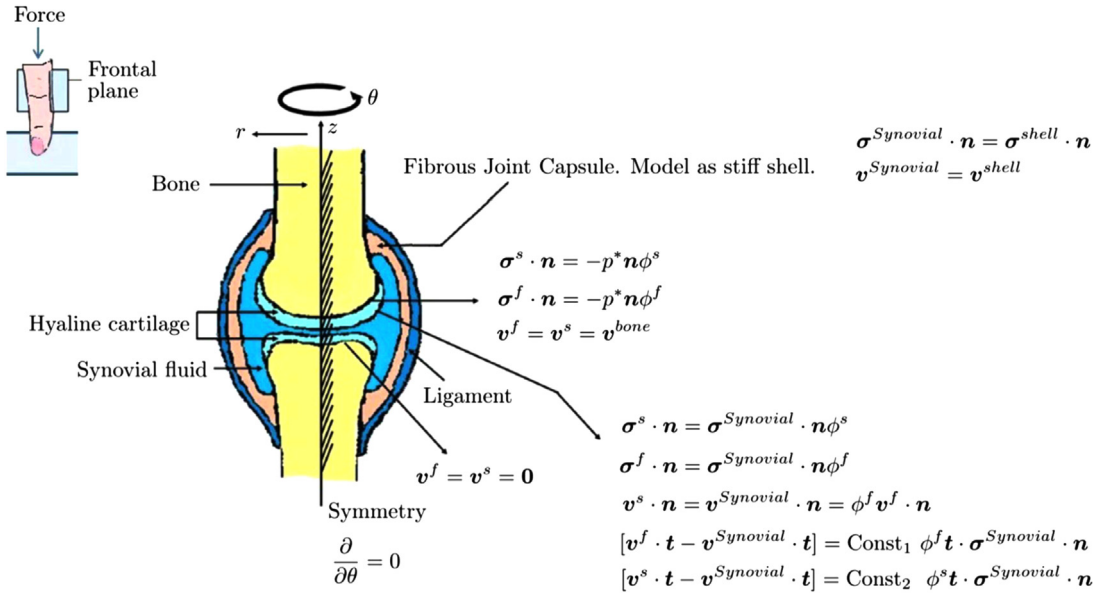

Fig. 3 – Boundary conditions for the finger knuckle, given axisymmetry approximations. The unit vectors n, t are normal and tangential to the interface where the boundary condition is imposed. The interpretation of p^{*} is discussed in the main text, whilst v^{bone} is an a-priori unknown for the very slow motion of the bone under forcing, for example pressing a finger against a solid surface with the knuckle straight. In addition, $\sigma^{Synovial}$, σ^{shell}, $v^{Synovial}$, v^{shell} are the stress and velocity fields of the synovial fluid and the fibrous capsule shell.

condition for the fluid phase mass balance hyperbolic partial differential equation is required. In addition, there are numerous further interfacial conditions for the finger cartilage in this model, as depicted in Fig. 3.

Cartilage-Bone: At the lower, assumed static, bone zero velocity for both fluid and solid phase is imposed,

$$\boldsymbol{v}^{\mathrm{f}}=\boldsymbol{v}^{\mathrm{s}}=\boldsymbol{0}.$$

On the upper bone-cartilage interface continuity of both velocity and stress for both phases are imposed, noting that the upper bone can move in response to the applied force, as represented by the pressure p^{*}. Thus firstly,

$$\boldsymbol{v}^{\mathrm{f}}=\boldsymbol{v}^{\mathrm{s}}=\boldsymbol{v}^{bone}.$$

In addition, on the upper bone-cartilage interface the stress from the synovial fluid must be distributed between the solid and fluid cartilage phases. In the absence of detailed empirical guidance, this is implemented via the area fractions of solid and fluid phase presenting at the bone-cartilage interface, though approximating collagen fibres as cylinders, these area fractions can readily be shown to be equivalent to volume fractions. For instance near bone, collagen fibres are essentially perpendicular to the interface, and for an array of N vertical cylinders of radius a, the ratio of surface area to volume fractions with a region of area A and height H is given by

$$\left(\frac{N\pi a^{2}}{A}\right)\left(\frac{HA}{NH\pi a^{2}}\right)=1.$$

Hence we have

$$\boldsymbol{\sigma}^{\mathrm{s}}\cdot\boldsymbol{n}=-p^{*}\boldsymbol{n}\phi^{\mathrm{s}},\quad \boldsymbol{\sigma}^{\mathrm{f}}\cdot\boldsymbol{n}=-p^{*}\boldsymbol{n}\phi^{\mathrm{f}}.$$

Cartilage-synovial fluid. At the cartilage-synovial interface, continuity of stress is imposed for both cartilage phases, again with area fractions taken as equivalent to volume fractions. Hence

$$\boldsymbol{\sigma}^{\mathrm{s}}\cdot\boldsymbol{n}=\boldsymbol{\sigma}^{Synovial}\cdot\boldsymbol{n}\phi^{\mathrm{s}},\quad \boldsymbol{\sigma}^{\mathrm{f}}\cdot\boldsymbol{n}=\boldsymbol{\sigma}^{Synovial}\cdot\boldsymbol{n}\phi^{\mathrm{f}}.$$

Additional conditions are required. Continuity of normal synovial fluid and normal solid cartilage velocity is imposed, $\boldsymbol{v}^{\mathrm{s}}\cdot\boldsymbol{n}=\boldsymbol{v}^{Synovial}\cdot\boldsymbol{n}$, representing a kinematic condition delimiting the evolution of the interface. We also have the cartilage fluid normal velocity and normal synovial fluid velocities are related by mass balance across the interface; assuming the cartilage fluid and synovial fluid have the same density, this is simply the constraint

$$\boldsymbol{v}^{Synovial}\cdot\boldsymbol{n}=\phi^{\mathrm{f}}\boldsymbol{v}^{\mathrm{f}}\cdot\boldsymbol{n}.$$

At this stage only tangential fluid velocities and tangential solid displacements, or alternatively tangential stresses, have not been subjected to boundary constraints. However, there are no fundamental principles for the imposition of these final boundary conditions and as we have discussed, even in simpler settings of a viscous fluid adjacent to a porous medium, which is effectively the biphasic model with an infinitely stiff solid phase, the most appropriate boundary condition is an open question (Le Bars and Worster, 2006). Nonetheless, it has been extensively studied by Beavers and Joseph (1967) in the context of the interface between a viscous fluid and a porous medium; their experimental study is consistent with a slip velocity, with the tangential fluid velocity proportional to the tangential stress, and is interpreted via a *boundary layer*, emphasising the importance of viscosity. Given the biphasic model is, in the limit of large stiffness of the solid component, a porous medium, the Beavers–Joseph boundary condition may be anticipated to be relevant in at least some regions of parameter space for the poroelastic multiphase models used to represent cartilage.

The absence of evidence-based tangential boundary conditions entails that characterising shear flows above cartilage would be a fruitful area for experimental investigation and modelling validation, not least because of the potential impact in understanding flow in joints and cartilage tribology. In the meantime we simply suggest tangential fluid velocity boundary conditions by analogy with the Beavers–Joseph condition, noting that the Beavers–Joseph experiments were conducted with constant volume fractions; hence we also explicitly partition the synovial fluid tangential stress by volume fraction. This gives

$$[\boldsymbol{v}^{\mathrm{f}} \cdot \boldsymbol{t} - \boldsymbol{v}^{Synovial} \cdot \boldsymbol{t}] = \mathrm{Const}_1 \phi^{\mathrm{f}} \boldsymbol{t} \cdot \boldsymbol{\sigma}^{Synovial} \cdot \boldsymbol{n},$$

$$[\boldsymbol{v}^{\mathrm{s}} \cdot \boldsymbol{t} - \boldsymbol{v}^{Synovial} \cdot \boldsymbol{t}] = \mathrm{Const}_2 \phi^{\mathrm{s}} \boldsymbol{t} \cdot \boldsymbol{\sigma}^{Synovial} \cdot \boldsymbol{n},$$

with two positive constants of proportionality where the $\boldsymbol{t}$ is the unit tangent to the interface, see Fig. 3. More generally, it is apparent that these tangential boundary conditions are effectively constitutive, and require empirical investigation.

3.4. *Further multiphase models*

The biphasic and triphasic modelling framework considered above, has not covered all types of cartilage multiphase models and, in particular, there is still a neglect of the impact that anisotropic and heterogeneous microstructure imposes on cartilage mechanics. Thus we proceed to review further multiphase models, especially those developing a framework for considering cartilage microstructure, though we do not present derivations of these diverse modelling frameworks in detail.

3.4.1. *Biphasic models of solid and ions*

A different type of biphasic model, with solid and ionic constituents, was recently proposed by Nagel and Kelly (2010). They considered an equilibrium model adjusted for fibre anisotropy, including a deterministic fibre angle orientation law according to Benninghoff-type architecture. This allowed a focussed study of the interaction of ions and the solid phase, for instance predicting that osmotic swelling causes pre-tension of fibres in cartilage tissue.

3.4.2. *Cellular inclusions*

The idea of the role of individual chondrocytes on tissue response can be traced back to two independent studies by Wu et al. (1999) and Guilak and Mow (2000) and this has been further developed by Federico et al. (2004, 2005), resulting in a very different modelling approach than the multiphasic theories. Particularly, Ferderico et. al. were initially motivated by the presence of significantly softer chondrocytes within cartilage tissue and wanted to study consequences of such structure on material behaviour. They used the upscaling method of homogenisation, with spherical inclusions, and hence their mixture quantities are directly related to mechanical properties on a finer scale; at least in terms of matrix and cell constituents this is probably the closest representation of microstructure in a cartilage modelling framework (Federico et al., 2004).

3.4.3. *Multiphase models with anisotropy and heterogeneity*

The impact of structural anisotropy and heterogeneity has been considered by Wilson et al. (2005a,b, 2006, 2007), building upon a triphasic framework where the ionic concentration is in local equilibrium, thus removing the need to explicitly track the ionic phase, analogous to our example above. However, the details differ and these papers introduced 'replaced pressures' with an electro-chemical potential, which includes the impact of the Donnan osmotic pressure and fixed charge density (FCD).

In particular Wilson et al. (2005a,b) compared their model with a triphasic finite element study under confined compression and 1D swelling, demonstrating that the assumption of ionic equilibrium generates an accurate approximation to the full triphasic model under these experimental conditions, illustrating the scope for controlled model simplification in focussed studies. Furthermore, this modelling framework was subsequently used as a building block to explore the impact of cartilage structure in more detail, for instance with Wilson et al. (2005a,b) exploring the impact of anisotropic collagen structure. Here, the non-fibrillar part of the cartilage solid matrix was treated as a neo-Hookean material with fibril-reinforcement, defined *in the context of cartilage* to entail that stress is distributed among fibres based on volume fraction, with stress in individual fibres related to the overall stress in the fibres via fibril density. In (Wilson et al., 2006) the authors furthered their goal of relating structure to cartilage behaviour, deriving a relation between permeability and tissue composition together with a proposed, new viscoelastic law for the fibrils. In a further generalisation, this group (Wilson et al., 2007) considered intra-and -extra fibrillar water content in order to correct for the effective fixed charge density, and the influence of the solid fraction on the compressive properties of the tissue. It was shown that with this model the typical depth-dependent behaviour of articular cartilage can be captured simply by the depth-dependence of the composition and collagen orientation only, with homogeneous material constants for the individual components.

More generally, many recent models have made advances towards the required levels of structural realism. Further notable examples of such advances include non-uniform distributions of fixed charge density (Chen et al., 2006), continuous fibre angular distribution swelled by the osmotic pressure of the proteoglycan ground matrix (Ateshian et al., 2009), alternative studies of depth-dependent collagen content, fibril orientation, fixed charge density and water content (Julkunen et al., 2008), and anisotropic diffusion (Pierce et al., 2013).

4. Moving towards modelling cartilage pathology such as osteoarthritis

We have briefly reviewed frameworks for multiphase cartilage modelling including their boundary conditions together with a description of common frameworks and ways of incorporating various aspects of the anisotropic and heterogeneous structure of cartilage. There is tremendous scope for such models to explore both homeostasis and disease. This

may include relatively simple tasks such as calculating solid stress, and therefore susceptibility to damage, with structural changes such as degradation/depletion of aggrecan or reconfiguration of the collagen meshwork. More elaborate programmes of work may calculate damage progression and feedbacks for matrix turnover, couple tissue changes that drive progression, or develop key structural markers of functionality or defunctionalisation that can be used to inform and assess treatment. The proliferation of modelling frameworks to explore structure-function relationships in detail, and the need to push parameter space into pathological regimes, emphasises the need to further validate and test the modelling frameworks.

This in turn presents many challenges and opportunities, which we develop below. In particular, to move focus from simulating and understanding bulk cartilage behaviour to developing insight of disease processes, we increasingly rely on our models to represent the functional interdependence of constituents, and to provide insight at the levels of structural hierarchy that represents degradative change. This is a more demanding objective than representing normal cartilage function in silico and would benefit from the ability to differentiate between modelling frameworks, a higher level of confidence in the modelling predictions, especially within pathological regions of parameter space, and a greater understanding of how modelling predictions can fail. All of these requirements assert the importance of model parameter estimation, testing and validation, including the extreme regimes of pathology.

Thus we proceed to discuss the difficulties, and also the opportunities such considerations present, in terms of combining mechanical measurements with recent developments in cartilage imaging, modelling, systems biology and mathematical upscaling tools, which determine macroscale behaviours from microscale information.

4.1. *Constitutive relations and model parameters*

Generally, the solid phase of cartilage is assumed to be *hyperelastic*, allowing the stress to be expressed via the free energy (Gurtin et al., 2010). It is also typically inferred that cartilage anisotropy arises primarily from collagen (Bachrach et al., 1998): numerous recent modelling studies use an isotropic hyperelastic contribution to the stress supplemented by an anisotropic contribution aligned with the local collagen fibril orientation (Wilson et al., 2005a,b, 2006, 2007; Pierce et al., 2009; Julkunen et al., 2013; Pierce et al., 2013). It is unclear, however, whether this is sufficient to describe pathology. It should be also noted that the choice of the bulk collagen strain energy potential cannot currently be directly verified or compared to experimental data (Federico and Gasser, 2010).

In contrast to the solid phase, constitutive relations for the fluid phase and the inter-phase drag are generally linear, as readily justified by maintaining model tractability and the absence of evidence to the contrary. There is also the possibility of constitutive coupling relations between stresses and solutes (Huyghe et al., 2009) whilst the tangential boundary conditions at the interface of fluid and cartilage are not characterised.

Further difficulties arise with identifiability, as similar findings emerge from very different models. For instance homogeneous equilibrium triphasic models (Ateshian et al., 2009) yield the same 'experimental behaviour' as inhomogeneous models (Federico et al., 2004), whilst even basic parameters such as Poisson's ratio are likely to be highly variable in cartilage (Wilson et al., 2007), due to its multiple phases, again hindering definitive parameter estimation. Thus resolving parameters is not straightforward, reducing confidence in extrapolating simulations to pathological regions of parameter space.

Furthermore, testing a detailed, many-parameter model against a small number of quasi-steady state axial loading curves is unlikely to be sufficient for model validation although some works are proposing ways to tackle this issue (Pierce et al., 2009); this also becomes even more prominent when considering pathological regimes as corresponding parameter values are not a straightforward extrapolation of the physiological ones. Nonetheless, predictions of the structural response to load are at hand in many models and to move the field forward, these should be confronted with complex reality and we thus proceed to discuss experimental interrogations that can potentially be used for such modelling development.

4.2. *Experimental frameworks for model validation and testing*

As described above, the advancement of our understanding of fundamental function, and its changes/roles in pathogenesis, requires the stronger coupling of theoretical and experimental approaches to characterisation. This may take the form of testing and improving the basic assumptions of classical models in the pathological regime, for example the potential breakdown of the biphasic model at the large strains and therefore low fluid fraction (see Section 3.1.2) that may occur with physiological loading in the highly permeable, aggrecan depleted matrix of diseased tissue. Experiments, particularly on diseased tissue, further challenge and refine boundary conditions, such as that of the impermeable cartilage-bone interface (Section 3.3).

Increased modelling sophistication such as the inclusion of collagen fibril anisotropy and 'reinforcement' detailed in Section 3.4.3, brings a need, and opportunity, to compare and optimise against experimental observations of that behaviour under load (e.g. Fig. 4. Bringing detailed theoretical predictions together with similarly detailed experimental measurements, outlined below, provides a basis to validate and improve constitutive model formulation, for example through controlled enzymatic digestions of matrix components, and then to explore disease-related changes such as calcification, decreased interconnectivity of collagen and therefore defunctionalisation of aggrecan entrapment, and heterogeneous patterns of degradation that can challenge or expand existing theories of pathogenesis. Importantly, by validating against cross-sectional data from different stages of the disease process, such models will be empowered to examine *processes* which are generally inaccessible to the experimentalist.

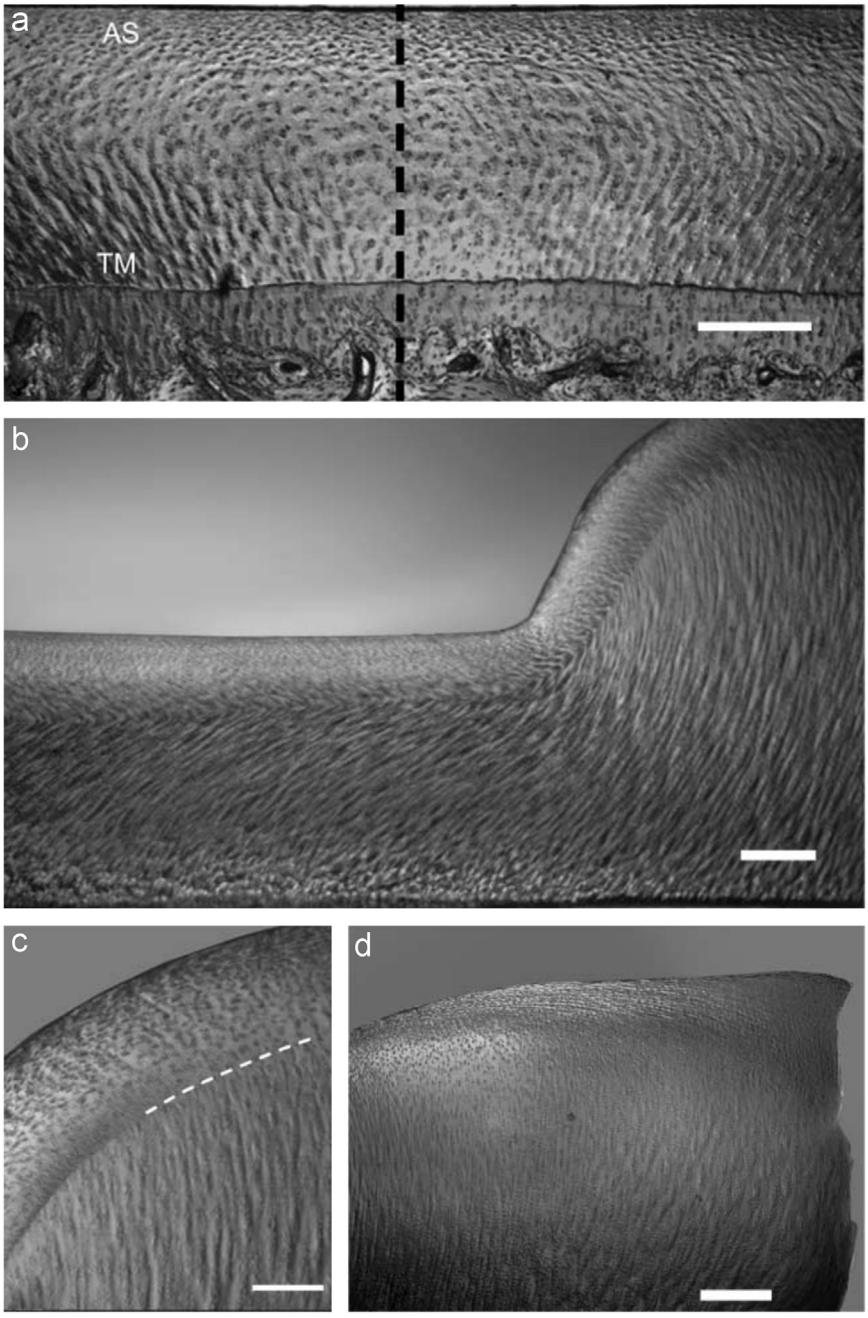

Fig. 4 – The complex restructuring of the collagen meshwork under static indentation, where the observed directionality from differential interference contrast (DIC) imaging corresponds to the dominant orientation of the collagen meshwork within a focal volume (≈1 μm diameter) in the loaded state. (A) A typical pattern of orientation near the symmetry axis (dashed vertical line) of an axisymmetric loading. AS=articular surface; TM=tidemark, (the transition between calcified and uncalcified cartilage); subchondral bone can be observed at the bottom of the image. (B–D) Collagen reorientation due to applied deformation extends laterally into the edge effect region and beyond, with a distinct reversal of shear observed at approximately 300 μm from the surface (dashed line in (C)). Image reproduced from (Thambyah and Broom, 2006), with permission. Scale bars = 200 μm (A, B, D); 100 μm (C).

There are three main approaches that can be used to probe the structural response to loading for such explorations. The first, used by the Broom group (Thambyah and Broom, 2006), involves static indentation to equilibrium, at which point the sample is immersed in fixative, typically overnight. The fixed tissue is then removed and sectioned for imaging in its deformed state (this was the method used for Fig. 4. This approach has the advantage of experimental ease, though it does not allow the structure to be probed before loading, and fixation limits the use of some measurements. A second approach is to use a plane-strain experiment in which a thin sample is clamped between glass plates to allow imaging during deformation. This more difficult technique allows real-time probing of structural changes with

deformation and loading, providing dynamical information and a richer dataset. A plane-strain experiment will be particularly useful for understanding transients and cyclical loading, load sharing between superficial and deeper layers, and the role of the chondron in protecting chondrocytes from stresses during loading. 2-D tensile measurements coupled with structural imaging can further provide information on constituent interactions and structure–function relationships in the tissue (Broom and Oloyede, 1993; Broom and Silyn-Roberts, 1989). Finally, cartilage-on-bone explants can be mechanically tested under magnetic resonance imaging (MRI) using non-metallic components in a pneumatic or hydraulic loading system (Wellard et al., 2014). Like plane-strain loading, this is experimentally difficult to set up, yet can provide rich 3-D data. Based on such approaches, we thus provide an overview of available techniques to extract and quantify the response of collagen, aggrecan and interstitial fluid to load.

4.2.1. *Collagen*

Collagen organisation can be measured quantitatively using a number of methods. The simplest and most accessible is polarised light microscopy (PLM, Bullough and Goodfellow, 1968) which gives information on anisotropy and orientation of scatterers, averaged within the focal volume, which is usually on the scale of a micron. Second harmonic generation (SHG) microscopy also provides this information, but is more specific to collagen due to the requirement of noncentrosymmetry (Freund et al., 1986). In particular SHG provides a powerful method for probing collagen structural changes with disease and deformation due to its sensitivity to fibril bundling, and can therefore provide quantitative and qualitative measures of early-stage disease over a number of hierarchical levels (Brown et al., 2014).

Vibrational spectroscopic methods can be used to estimate the concentration of collagen in a bulk sample, or to determine its distribution when used as imaging techniques (Camacho et al., 2001; Dehring et al., 2006). Coupled with polarisation optics, these methods reveal the orientation of matrix components as well as concentrations. The choice between infrared, Raman or near-infrared requires a balancing of each method's strengths and weaknesses. Infrared spectroscopy is easy to interpret and well-suited to imaging, however the low penetration (few tens of micrometres) in tissue limits its use in bulk measurements. Raman spectroscopy is highly penetrating and easy to interpret, but requires long integration times (approximately one photon per million is Raman scattered in standard setups). Near infrared spectroscopy is fast and penetrating, though difficult to interpret due to wide, overlapping absorbance bands. A more powerful, but less accessible, technique for unfixed samples is small angle X-ray scattering (SAXS), which is sensitive to collagen D-spacing (often referred to as banding, typically $\approx$67 nm), and can therefore be used to directly measure average orientation and, most importantly, strain in collagen fibrils within the focal volume of the X-ray beam (Moger et al., 2007).

Such techniques can thus provide detailed collagen information, including orientation, potentially allowing a careful parametrisation and model testing for the solid phase of cartilage, including extensions from simple isotropic solid phase models to more complex anisotropic mechanical models.

4.2.2. *Aggrecan*

Aggrecan is trapped within the collagen meshwork and will therefore move with collagen during deformation. It remains, however, an important component to measure in order to test the effects of structural changes in early-stage osteoarthritis. As collagen and aggrecan are functionally interdependent, the effects of aggrecan depletion on local mechanics and collagen restructuring under load is important in understanding the disease process. Recent work using scanning probe techniques (Dean et al., 2006) has measured compressive properties of opposing aggrecan macromolecules within 0.001–1 NaCl solutions (Fig. 5). Coupled with shear information (Han et al., 2007) and constraining collagen–aggrecan adhesion forces (Rojas et al., 2014), this provides an experimental basis for building microstructurally relevant constitutive equations.

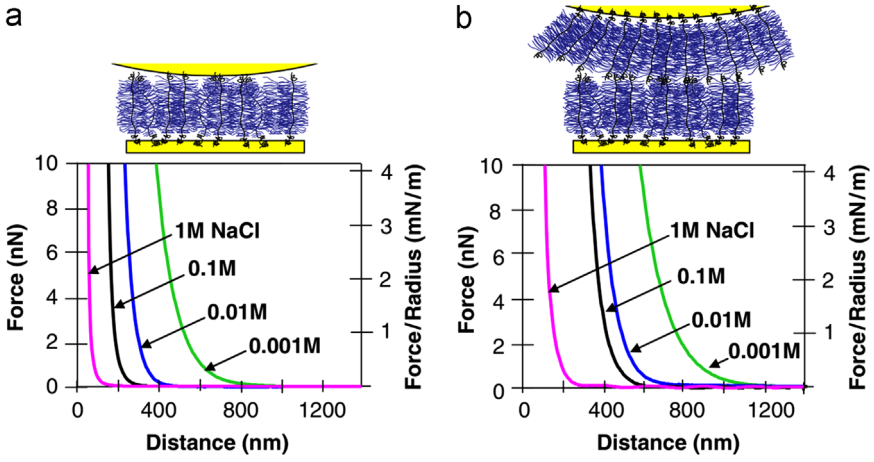

Fig. 5 – Compressive forces between (a) a 2.5 mm radius tip and a single aggrecan layer attached to the substrate; and (b) opposing aggrecan layers attached to both the tip and substrate, in different bath ionic strengths (0.001 – – 1 M NaCl). Reprinted from (Dean et al., 2006), with permission from Elsevier (3662880049459).

Staining with safranin-O and digital densitometry (Kiraly et al., 1996) can be used to measure the distribution of aggrecan on larger scales. Similar information can be gained using vibrational spectroscopy (Camacho et al., 2001), also enabling the tracking of concentrations under plane strain experiments, in turn allowing aggrecan content and its effects to be parametrised and modelled. Coupling aggrecan measurements with the use of external salt baths allows scope for measuring the mechanical and structural impact of ion concentration changes, thus enabling parametrisation and the possibility of testing appropriate modelling frameworks for the stress due to charges.

4.2.3. *Fluid*

Bulk fluid pressure measurements, coupled with mechanical measurements, have been available for some time and provide a useful tool for describing the role of interstitial fluid pressurisation in load carriage and lubrication (Soltz and Ateshian, 1998). Fluid interaction with the cartilage surface may also further be explored with fluid shearing techniques (Beavers and Joseph, 1967), whilst MRI provides 0.1–0.5 mm resolution of solute transport (Burstein et al., 1993) and relative permeability (Filidoro et al., 2005). Permeability measurements by diffusion tensor imaging, require long times and high fields, yet provide crucial data. The permeability tensor, and its change with loading, depends on the configuration of collagen and aggrecan and is likely to be an important functional change early in osteoarthritic progression, as higher permeability will transfer stress to the solid matrix more quickly, arguably increasing susceptibility to further damage. T2, T2* and exchange measurements, which are sensitive to water confinement in the matrix and its binding to aggrecan, can potentially provide similar information over much shorter timescales. Like diffusion, these measurements are best suited to equilibrium but nonetheless have potential for the testing and validation of cartilage models.

4.3. *Modelling developments: current and future*

With all these empirical interrogations, there remain fundamental difficulties in that experimental changes affect many aspects of cartilage in a highly coupled manner. Thus in generality one cannot isolate a given parameter to allow simple testing of a model response. First, an adaptable modelling simulation environment is required, so that parameter farms of simulations varying a host of cartilage properties can be quickly implemented to facilitate model testing, analogous to the open-source CMiSS human physiome suite (Bradley, 2011). Indeed, recently, Ateshian et al. (2011, 2013) have provided an open-source numerical environment, FEBio, using finite element methods and specifically targeting continuum soft tissue modelling, such as cartilage. In particular, this numerical environment is specifically designed for soft tissue, for instance allowing phenomena such as permeation, osmosis, electroosmosis, diffusion, electrophoresis and barophoresis to be considered more readily than generic, commercial finite element packages. Such developments will facilitate the testing of parameters and concepts in modelling studies, which in turn will facilitate the detailed coupling of modelling with the information emerging from the above imaging and mechanical studies.

Furthermore, determining the links between microstructure and bulk properties is a fundamental multiscale problem that permeates through extensive areas of applied mathematics. In particular, and in contrast to most of the studies described above, we note that there are averaging techniques to consider the mass and concentration balance equations for cartilage at the microlevel and, at least prospectively, to then scale to the bulk level (Davit et al., 2010; Cushman et al., 2002). Ultimately these raise the prospect of exploiting the detailed microstructural information that the above imaging tools are capable of delivering for incorporation into models. In turn, this would allow the consequences of microstructural changes to be explored in simulations without the need to consider multiple orders of lengthscale (Davit et al., 2013), with the one example for cartilage given by Federico et. al.'s upscaling studies of how the presence of cartilage cells, chondrocytes, impacts macroscale mechanics (Federico et al., 2004, 2005).

Even with such possibilities, exploiting experimental data to distinguish modelling and parameter choices is still not straightforward. Nonetheless, numerous system biological tools have been developed for such parametrisation problems, especially by classifying the relative importance of parameters taking into account interactions between multiple simultaneous changes. These global sensitivity analyses can proceed via numerous statistical or machine learning techniques, such as least square general linear methods (Makler-Pick et al., 2011), or Latin hypercube sampling and partial rank correlations (Wu et al.,), or recursive partitioning tools such as random forests (Strobl et al., 2009). In particular, such techniques facilitate at least the prospect of reducing the combinatorial difficulties of investigating parameter estimation and validation across extensive parameter spaces regions.

4.4. *Extending models to pathology, ageing and select interventions*

Known processes associated with cartilage disease involve phenomena such as aggrecan depletion, collagen meshwork restructuring, subchondral bone changes and advancing calcification, whereas ageing induces changes such as increased cross linking and aggrecan degradation. Treatments such as osteotomy aim to modulate the mechanical environment of the tissue to halt or slow disease progression, while others seek to recreate the structure and function of native tissue in engineered constructs for localised replacement. As mentioned above, extending models into such regions of parameter space to simulate pathology and ageing, and thus also potential compensating interventions, requires confidence in the constitutive relations and modelling frameworks, even with simple generalisations of functional models such as the impact of aggrecan depletion.

Nonetheless, these raise numerous prospective topics for exploration within virtual cartilage models. For instance, one could assess how lubrication processes and stresses are altered in cartilage with degradative changes, such as surface disruption, synovial fluid changes, or aggrecan depletion or

assess how subchondral bone lesions and the advancing calcification front affect stress distributions in the overlying cartilage. Cartilage models can also provide insight into treatment effects as highlighted by considering the impact of interventions such as osteotomy or bracing on the stress distribution within cartilage. In particular the extent to which such interventions may disperse stresses from cartilage lesions is of current interest as clinicians attempt to provide solutions to the 'treatment gap' between the onset of pain and/or disability, and the applicability of successful late-stage treatments such as joint replacement.

5. Summary and conclusions

We have summarised the assumptions underlying, and the construction processes defining, core models of cartilage mechanics, with a hierarchy of complexity from the simplest biphasic model to modern extensions of the triphasic models taking into account numerous aspects of cartilage structure and physiology, such as the depth dependent distribution of collagen fibre orientation, aggrecan density and structural anisotropies. However, this level of complexity, coupled with the currently limited resolving power of small numbers of quasi-steady state axial loading curves, entails that model parametrisation and validation is under developed. In addition, modelling in the field has not embraced the complex geometry of a joint, nor the interfacial mechanics of cartilage and synovial fluid, despite the fact the drainage routes are critical in the physical mechanism of joint lubrication and a subject of debate in the literature. Consequently, there are still numerous topics to explore even in the modelling of function, though arguably the most important of these is to continue current efforts to parametrise and validate cartilage models, including their boundary conditions.

Furthermore, combining modern imaging technologies with the fixing of loaded samples or the temporal evolution of loading experiments can offer substantial new data on the solid, fluid and ionic phases of cartilage, as well as its anisotropies thus potentially facilitating model parametrisation, including the constitutive relations. Pursuing these directions will most likely exploit recent efforts to provide an open-source modelling suite for cartilage simulations, FEBio, together with the hijacking of modern systems biology tools, based on statistical and machine learning algorithms, to provide the modelling capabilities required for high dimensional parametrisation. This in turn also offers the prospect of further investigations of such models, exploring regions of parameter spaces corresponding to ageing, pathology and intervention, such as aggrecan degradation, collagen restructuring and the performance of prospective engineered tissue. More generally, such directions may improve our systems level understanding of cartilage and how its various constituents orchestrate, in health to provide remarkable mechanical performance and in pathology, to provide insight into joint dysfunction and prospective treatment.

Acknowledgements

E.A.G. and V.K. gratefully acknowledge support from the EPSRC platform grant, EP/I01893X/1.Y-C.C. and C.P.B acknowledge support from Orthopaedic Research UK (ref 504), the Taiwan Government Scholarship to Study Abroad (GSSA), Arthritis Research UK (grant 20299 and Oxford EOTC), Marie Curie IRSES (skelGEN), and the Oxford NIHR BRU in musculoskeletal disease.

Appendix A. Supplementary material

Supplementary data associated with this article can be found in the online version at http://dx.doi.org/ 10.1016/j.jmbbm.2016.04.032.

REFERENCES

Ateshian, G., 2007a. On the theory of reactive mixtures for modeling biological growth. Biomech. Model. Mechanobiol. 6 (6), 423–445.
Ateshian, G., 2007b. Anisotropy of fibrous tissues in relation to the distribution of tensed and buckled fibers. J. Biomech. Eng. 129 (2), 240–249.
Ateshian, G., 2009. The role of interstitial fluid pressurization in articular cartilage lubrication. J. Biomech. 42, 1163–1176.
Ateshian, G., Lai, W., Zhu, W., Mow, V., 1994. An asymptotic solution for the contact of two biphasic cartilage layers. J. Biomech. 27 (11), 1347–1360.
Ateshian, G., Warden, W., Kim, J., Grelsamer, R., Mow, V., 1997. Finite deformation biphasic material properties of bovine articular cartilage from confined compression experiments. J. Biomech. 30, 1157–1164.
Ateshian, G., Chahine, N., Basalo, I., Hung, C., 2004. The correspondence between equilibrium biphasic and triphasic material properties in mixture models of articular cartilage. J. Biomech. 37 (3), 391–400.
Ateshian, G., Rajan, V., Chahine, N., Canal, C., Hung, C., 2009. Modeling the matrix of articular cartilage using a continuous fiber angular distribution predicts many observed phenomena. J. Biomech. Eng. 131 (6), 061003.
Ateshian, G., Albro, M., Maas, S., Weiss, J., 2011. Finite element implementation of mechanochemical phenomena in neutral deformable porous media under finite deformation. J. Biomech. Eng. 133 (8), 081005.
Ateshian, G., Maas, S., Weiss, J., 2013. Multiphasic finite element framework for modeling hydrated mixtures with multiple neutral and charged solutes. J. Biomech. Eng. 135 (11), 111001.
Athanasiou, K., Darling, E., Hu, J., DuRaine, G., Hari Reddi, A., 2013. Articular Cartilage. CRC Press, Boca Raton, FL.
Atkin, R., Craine, R., 1976. Continuum theories of mixtures: basic theory and historical development. Q. J. Mech. Appl. Math. 29 (2), 209–244.
Bachelor, G., 2000. An Introduction to Fluid Dynamics. Cambridge University Press, New York, USA.
Bachrach, N., Mow, V., Guilak, F., 1998. Incompressibility of the solid matrix of articular cartilage under high hydrostatic pressures. J. Biomech. 31 (5), 445–451.
Basser, P., Grodzinsky, A., 1993. The Donnan model derived from microstructure. Biophys. Chem. 46, 57–68.
Beavers, G., Joseph, D., 1967. Boundary conditions at a naturally permeable wall. J. Fluid Mech. 30, 197–207.

Bedford, A., Drumheller, D., 1983. Theories of immiscible and structured mixtures. Int. J. Eng. Sci. 21 (8), 863–960, http://dx.doi.org/10.1016/0020-7225(83)90071-X.
Bennethum, L.S., Cushman, J.H., 2002. Multicomponent, multiphase thermodynamics of swelling porous media with electroquasistatics: I. macroscale field equations. Transp. Porous Media 47, 309–336.
Benninghoff, A., 1925. Form und bau der Gelenknorpel in ihren Bezeihungen zur Funktion. Forschung 2 (2), 783–825.
Bercovici, D., Ricard, Y., Schubert, G., 2001. A two-phase model for compaction and damage. i- general theory. J. Geophys. Res. 106 (B5), 8887–8906.
Biot, M., 1941. General theory of three-dimensional consolidation. J. Appl. Phys. 12 (2), 155–164.
Bowen, R., 1976. Theory of mixtures. In: A.C. Eringen (Ed.), Continuum Physics.
Bowen, R., 1980. Incompressible porous media models by use of the theory of mixtures. Int. J. Eng. Sci. 18 (9), 1129–1148.
Bradley, C., Bowery, A., Britten, R., Budelmann, V., Camara, O., Christie, R., Cookson, A., Frangi, A., Gamage, T., 2011. OpenCMISS: a multi-physics and multi-scale computational infrastructure for the VPH/Physiome project. Progress. Biophys. Mol. Biol. 107 (1), 32–47.
Broom, N., Oloyede, A., 1993. Experimental-Determination Of The Subchondral Stress-Reducing Role Of Articular-Cartilage Under Static And Dynamic Compression. Clin. Biomech. 8 (2), 102–108.
Broom, N., Silyn-Roberts, H., 1989. The three-dimensional 'knit' of collagen fibrils in articular cartilage. Connect. Tissue Res. 23, 261–277.
Brown, C., Houle, M., Popov, K., Nicklaus, M., Couture, C., Laliberte, M., Brabec, T., Ruediger, A., Carr, A., Price, A., Gill, H., Ramunno, L., Legare, F., 2014. Imaging and modeling collagen architecture from the nano to micro scale. Biomed. Opt. Express 5 (1), 233–243.
Bullough, P., Goodfellow, J., 1968. The significance of the fine structure of articular cartilage. J. Bone Joint Surg. 50-B (4), 852–857 British Volume.
Burstein, D., Gray, M., Hartman, A., Gipe, R., Foy, B., 1993. Diffusion of small solutes in cartilage as measured by nuclear magnetic resonance (NMR) spectroscopy and imaging. J. Orthop. Res. 11 (4), 465–478.
Buschmann, M., Grodzinsky, A., 1995. A molecular-model Of proteoglycan-associated electrostatic forces In cartilage mechanics. J. Biomech. Eng. -Trans. ASME 117 (2), 179–192.
Camacho, N., West, P., Torzilli, P., Mendelsohn, R., 2001. Imaging of collagen and proteoglycan in bovine cartilage. Biopolymers 62 (1), 1–8.
Chandesris, M., Jamet, D., 2006. Boundary conditions at a planar fluid-porous interface for a poiseuille flow. Int. J. Heat. Mass. Transf. 49 (13), 2137–2150.
Chen, Y., Chen, X., Hisada, T., 2006. Non-linear finite element analysis of mechanical electrochemical phenomena in hydrated soft tissues based on triphasic theory. Int. J. Numer. Methods Eng. 65 (2), 147–173.
Coleman, B., Noll, W., 1963. The thermodynamics of elastic materials with heat conduction and viscosity. Arch. Ration. Mech. Anal. 13 (1), 167–178.
Corry, B., Kuyucak, S., Chung, S., 2000. Tests of continuum theories as models of ion channels. II. Poisson-Nernst-Planck theory versus Brownian dynamics. Biophys. J. 78 (5), 2364–2381.
Cushman, J., Bennethum, L., Hu, B., 2002. A primer on upscaling tools for porous media. Adv. Water Resour. 25 (8–12), 1043–1067.
Davit, Y., Byrne, H., Osborne, J., Pitt-Francis, J., Gavaghan, D., Quintard, M. Hydrodynamic dispersion within porous biofilms. Phys. Rev. E 87 (1), 2013.
Davit, Y., Debenest, G., Wood, B., Quintard, M., 2010. Modeling non-equilibrium mass transport in biologically reactive porous media. Adv. Water Resour. 33 (9), 1075–1093.
de Boer, R., 2005. Trends in Continuum Mechanics of Porous Media. Springer, Dordrecht, The Netherlands.
Dean, D., Han, L., Grodzinsky, A.J., Ortiz, C., 2006. Compressive nanomechanics of opposing aggrecan macromolecules. J. Biomech. 39 (14), 2555–2565.
Dehring, K.A., Smukler, A.R., Roessler, B.J., Morris, M.D., 2006. Correlating changes in collagen secondary structure with aging and defective type ii collagen by raman spectroscopy. Appl. Spectrosc. 60 (4), 366–372.
Dell'Isola, F., Madeo, A., Seppecher, P., 2009. Boundary conditions at fluid-permeable interfaces in porous media: A variational approach. Int. J. Solids Struct. 46 (17), 3150–3164.
Ehlers, W., 2002. Foundations of Multiphasic and Porous Materials. Springer.
Elkin, B., Shaik, M., Morrison, B., 2010. Fixed negative charge and the donnan effect: a description of the driving forces associated with brain tissue swelling and edema. Phil. Trans. R. Soc. A 368, 585–603.
Federico, S., Gasser, T., 2010. Nonlinear elasticity of biological tissues with statistical fibre orientation. J. R. Soc. Interface 7 (47), 955–966.
Federico, S., Herzog, W., 2008. On the anisotropy and inhomogeneity of permeability in articular cartilage. Biomech. Model. Mechanobiol. 7 (5), 367–378.
Federico, S., Grillo, A., Herzog, W., 2004. A transversely isotropic composite with a statistical distribution of spheroidal inclusions: a geometrical approach to overall properties. J. Mech. Phys. Solids 52 (10), 2309–2327.
Federico, S., Grillo, A., La Rosa, G., Giaquinta, G., Herzog, W., 2005. A transversely isotropic, transversely homogeneous microstructural-statistical model of articular cartilage. J. Biomech. 38 (10), 2008–2018.
Filidoro, L., Dietrich, O., Weber, J., Rauch, E., Oerther, T., Wick, M., Reiser, M., Glaser, C., 2005. High-resolution diffusion tensor imaging of human patellar cartilage: Feasibility and preliminary findings. Magn. Reson. Med. 53 (5), 993–998.
Freund, I., Deutsch, M., Sprecher, A., 1986. Connective tissue polarity. optical second-harmonic microscopy, crossed-beam summation, and small-angle scattering in rat-tail tendon. Biophys. J. 50 (4), 693–712.
Gleghorn, J., Bonassar, L., 2008. Lubrication mode analysis of articular cartilage using Stribeck surfaces. J. Biomech. 41 (9), 1910–1918.
Goldberg, I., Folk, R., 1988. Solutions for steady and nonsteady entrance flow in a semi-infinite circular tube at very low reynolds number. SIAM J. Appl. Math. 48 (4), 772–780.
Gray, W.G., Miller, C.T., 2005. Thermodynamically constrained averaging theory approach for modeling flow and transport phenomena in porous medium systems: 1. motivation and overview. Adv. Water Resour. 28, 161–180.
Gu, W., Lai, W., Mow, V., 1998. A mixture theory for charged-hydrated soft tissues containing multi-electrolytes: passive transport and swelling behaviors. J. Biomech. Eng. 120 (2), 169–180.
Guilak, F., Mow, V.C., 2000. The mechanical environment of the chondrocyte: a biphasic finite element model of cell-matrix interactions in articular cartilage. J. Biomech. 33 (12), 1663–1673.
Guo, H., Maher, S.A., Torzilli, P.A., 2014. A biphasic multiscale study of the mechanical microenvironment of chondrocytes within articular cartilage under unconfined compression. J. Biomech. 47 (11), 2721–2729.
Gurtin, M., Fried, E., Anand, L., 2010. The Mechanics and Thermodynamics of Continua. Cambridge University Press, New York, USA.

Halonen, K., Mononen, M., Jurvelin, J., Toyras, J., Korhonen, R., 2013. Importance of depth-wise distribution of collagen and proteoglycans in articular cartilage-A 3D finite element study of stresses and strains in human knee joint. J. Biomech. 46 (6), 1184–1192.

Han, L., Dean, D., Ortiz, C., Grodzinsky, A.J., 2007. Lateral nanomechanics of cartilage aggrecan macromolecules. Biophys. J. 92 (4), 1384–1398.

Harrigan, T., Mann, R., 1987. State variables for modelling physical aspects of articular cartilage. Int. J. Solids Struct. 23 (9), 1205–1218.

Hassanizadeh, S.J., Gray, W.C., 1979. General conservation equations for multi-phase systems: 1. averaging procedure. Water Resour. Res. 2, 131–144.

Hlavacek, M., 1993. The role of synovial-fluid filtration by cartilage in lubrication of synovial joints 2. Squeeze-film lubrication - homogeneous filtration. J. Biomech. 26 (10), 1151–1160.

Hou, J., Holmes, M., Lai, W., Mow, V., 1989. Boundary conditions at the cartilage-synovial fluid interface for joint lubrication and theoretical verifications. J. Biomech. Eng. 111 (1), 78–87.

Huyghe, J., Janssen, J., 1997. Quadriphasic mechanics of swelling incompressible porous media. Int. J. Eng. Sci. 35 (8), 793–802.

Huyghe, J., Wilson, W., Malakpoor, K., 2009. On the thermodynamical admissibility of the triphasic theory of charged hydrated tissues. J. Biomech. Eng. 131 (4), 044504.

Julkunen, P., Wilson, W., Jurvelin, J., Rieppo, J., Qu, C., Lammi, M., Korhonen, R., 2008. Stress-relaxation of human patellar articular cartilage in unconfined compression: prediction of mechanical response by tissue composition and structure. J. Biomech. 41 (9), 1978–1986.

Julkunen, P., Wilson, W., Isaksson, H., Jurvelin, J., Herzog, W., Korhonen, R., 2013. A review of the combination of experimental measurements and fibril-reinforced modeling for investigation of articular cartilage and chondrocyte response to loading. Comput. Math. Methods Med..

Karajan, N., 2012. Multiphasic intervertebral disc mechanics: theory and application. Arch. Comput. Methods Eng. 19 (2), 261–339.

Katta, J., Jin, Z., Ingham, E., Fisher, J., 2008. Biotribology of articular cartilage-A review of the recent advances. Med. Eng. Phys. 30 (SI 10), 1349–1363.

Kiraly, K., Lapvetelainen, T., Arokoski, J., Torronen, K., Modis, L., Kiviranta, I., Helminen, H., 1996. Application of selected cationic dyes for the semiquantitative estimation of glycosaminoglycans in histological sections of articular cartilage by microspectrophotometry. Histochem. J. 28, 577–590.

Klika, V., 2014. A guide through available mixture theories for applications. Crit. Rev. Solid State Mater. Sci. 39 (2), 154–174.

Lai, W., Hou, J., Mow, V., 1991. A triphasic theory for the swelling and deformation behaviors of articular cartilage. J. Biomech. Eng. 113 (3), 245–258.

Le Bars, M., Worster, M., 2006. Interfacial conditions between a pure fluid and a porous medium: implications for binary alloy solidification. J. Fluid Mech. 550, 149–173.

Lightfoot, E., Cussler, E., Rettig, R., 1962. Applicability of the Stefan–Maxwell equations to multicomponent diffusion in liquids. AICHE J. 8 (5), 708–710.

Makler-Pick, V., Gal, G., Gorfine, M., Hipsey, M., Carmel, Y. Sensitivity analysis for complex ecological models–a new approach. Environ. Model. Softw. 26 (2), 2011, 124-134.

Maroudas, A., 1976. Balance between swelling pressure and collagen tension in normal and degenerate cartilage. Nature 260, 808–809.

McCutchen, C., 1959. Sponge-Hydrostatic And Weeping Bearings. Nature 184 (4695), 1284–1285, http://dx.doi.org/10.1038/1841284a0.

Moger, C., Barrett, R., Bleuet, P., Bradley, D., Ellis, R., Green, E., Knapp, C., Muthuvelu, P., Winlove, C., 2007. Regional variations of collagen orientation in normal and diseased articular cartilage and subchondral bone determined using small angle X-ray scattering (SAXS). Osteoarthr. Cartil. 15 (6), 682–687.

Moo, E.K., Han, S.K., Federico, S., Sibole, S.C., Jinha, A., Osman, N. A.A., Pingguan-Murphy, B., Herzog, W., 2014. Extracellular matrix integrity affects the mechanical behaviour of in-situ chondrocytes under compression. J. Biomech. 47 (5), 1004–1013.

Mow, V., Kuei, S., Lai, W., Armstrong, C., 1980. Biphasic creep and stress relaxation of articular cartilage in compression: theory and experiments. J. Biomech. Eng. 102 (1), 73–84.

Mow, V., Kwan, M., Lai, W., Holmes M., 1986. A finite deformation theory for nonlinearly permeable soft hydrated biological tissues. In: G. Schmid-Schonbein, S.-Y. Woo, B. Zweifach (Eds.), Frontiers in Biomechanics, Springer, New York, pp. 153–179.

Mow, V., Gibbs, M., Lai, W., Zhu, W., Athanasiou, K., 1989. Biphasic indentation of articular-cartilage. 2. A numerical algorithm and an experimental-study. J. Biomech. 22 (8–9), 853–861.

Mow, V., Wang, C., Hung, C., 1999. The extracellular matrix, interstitial fluid and ions as a mechanical signal transducer in articular cartilage. Osteoarthr. Cartil. 7, 41–58.

Moy, G., Corry, B., Kuyucak, S., Chung, S., 2000. Tests of continuum theories as models of ion channels. I. Poisson-Boltzmann theory versus Brownian dynamics. Biophys. J. 78 (5), 2349–2363.

Müller, I., Ruggeri, T., 1998. Rational Extended Thermodynamics, vol. 37, Springer Verlag, New York.

Nagel, T., Kelly, D., 2010. The influence of fiber orientation on the equilibrium properties of neutral and charged biphasic tissues. J. Biomech. Eng. 132 (11), 114506.

Ng, L., Grodzinsky, A., Patwari, P., Sandy, J., Plaas, A., Ortiz, C., 2003. Individual cartilage aggrecan macromolecules and their constituent glycosaminoglycans visualized via atomic force microscopy. J. Struct. Biol. 143 (3), 242–257.

Oloyede, A., Broom, N., 1996. The biomechanics of cartilage load-carriage. Connect. Tissue Res. 34 (2), 119–143.

Pavelka, M., Maršík, F., Klika, V., 2014. Consistent theory of mixtures on different levels of description. Int. J. Eng. Sci. 78, 192–217.

Pierce, D.M., Trobin, W., Trattnig, S., Bischof, H., Holzapfel, G.A., 2009. A phenomenological approach toward patient-specific computational modeling of articular cartilage including collagen fiber tracking. J. Biomech. Eng. 131 (9), 091006.

Pierce, D., Ricken, T., Holzapfel, G., 2013. A hyperelastic biphasic fibre-reinforced model of articular cartilage considering distributed collagen fibre orientations: continuum basis, computational aspects and applications. Comput. Methods Biomech. Biomed. Eng. 16 (12), 1344–1361.

Quintard, M., Bletzacker, L., Chenu, D., Whitaker, S., 2006. Nonlinear, multicomponent, mass transport in porous media. Chem. Eng. Sci. 61 (8), 2643–2669.

Rajagopal, K., 2007. On a hierarchy of approximate models for flows of incompressible fluids through porous solids. Math. Model. Methods Appl. Sci. 17 (02), 215–252.

Rojas, F.P., Batista, M.A., Lindburg, C.A., Dean, D., Grodzinsky, A.J., Ortiz, C., Han, L., 2014. Molecular adhesion between cartilage extracellular matrix macromolecules. Biomacromolecules 15 (3), 772–780 pMID: 24491174.

Saffman, P., 1971. On the boundary condition at the interface of a porous medium. Stud. Appl. Math. 1, 93–101.

Setton, L.A., Elliott, D.M., Mow, V.C., 1999. Altered mechanics of cartilage with osteoarthritis: human osteoarthritis and an experimental model of joint degeneration. Osteoarthr. Cartil. 7 (1), 2–14.

Soltz, M., Ateshian, G., 1998. Experimental verification and theoretical prediction of cartilage interstitial fluid

pressurization at an impermeable contact interface in confined compression. J. Biomech. 31 (10), 927–934.
Soper, A., Benmore, C. Quantum differences between heavy and light water. Phys. Revi. Lett. 101 (6), 2008.
Strobl, C., Malley, J., Tutz, G., 2009. An Introduction to recursive partitioning: rationale, application, and characteristics of classification and regression trees, bagging, and random forests. Psychol. Methods 14 (4), 323–348.
Thambyah, A., Broom, N., 2006. Micro-anatomical response of cartilage-on-bone to compression: mechanisms of deformation within and beyond the directly loaded matrix. J. Anat. 209, 611–622.
Thurston, G.B., Greilin, H., 1978. Viscoelastic properties of pathological synovial fluids for a wide range of oscillatory shear rates and frequencies. Rheol. Acta 17, 433–445.
Travis, K., Todd, B., Evans, D., 1997. Poiseuille flow of molecular fluids. Phys. A 240 (1–2), 315–327.
Truesdell, C., 1984. Rational Thermodynamics. Springer-Verlag, New York.
Walker, P., Dowson, D., Longfield, M., Wright, V., 1968. Boosted lubrication In synovial joints by fluid entrapment and enrichment. Ann. Rheum. Dis. 27 (6)http://dx.doi.org/10.1136/ard.27.6.512 512–&.
Weiss, T., 1996. Cellular Biophysics. Transport, vol. 1. MIT Press.
Wellard, R., Ravasio, J., Guesne, S., Bell, C., Oloyede, A., Tevelen, G., Pope, J., Momot, K., 2014. Simultaneous magnetic resonance imaging and consolidation measurement of articular cartilage. Sensors 14, 7940–7958.
Wilmanski, K., 2008. Continuum Thermodynamics, Vol. I: Foundations. World Scientific, Singapore.
Wilson, W., van Donkelaar, C., van Rietbergen, B., Huiskes, R., 2005a. A fibril-reinforced poroviscoelastic swelling model for articular cartilage. J. Biomech. 38 (6), 1195–1204.
Wilson, W., Van Donkelaar, C., Huyghe, J., 2005b. A comparison between mechano-electrochemical and biphasic swelling theories for soft hydrated tissues. J. Biomech. Eng. 127 (1), 158–165.
Wilson, W., Huyghe, J., Van Donkelaar, C., 2006. A composition-based cartilage model for the assessment of compositional changes during cartilage damage and adaptation. Osteoarthr. Cartil. 14 (6), 554–560.
Wilson, W., Huyghe, J., Van Donkelaar, C., 2007. Depth-dependent compressive equilibrium properties of articular cartilage explained by its composition. Biomech. Model. Mechanobiol. 6 (1–2), 43–53.
Wu, J., Dhingra, R., Gambhir, M., Remais, J. Sensitivity analysis of infectious disease models: methods, advances and their application. J. R. Soc. Interface 10 (86). http://dx.doi.org/10.1098/rsif.2012.1018.
Wu, J., Herzog, W., Epstein, M., 1999. Modelling of location-and time-dependent deformation of chondrocytes during cartilage loading. J. Biomech. 32 (6), 563–572.